



Universiteit
Leiden
The Netherlands

Primary T-cell responses against SARS-CoV-2 in patients with hematological disorders

Pothast, C.R.

Citation

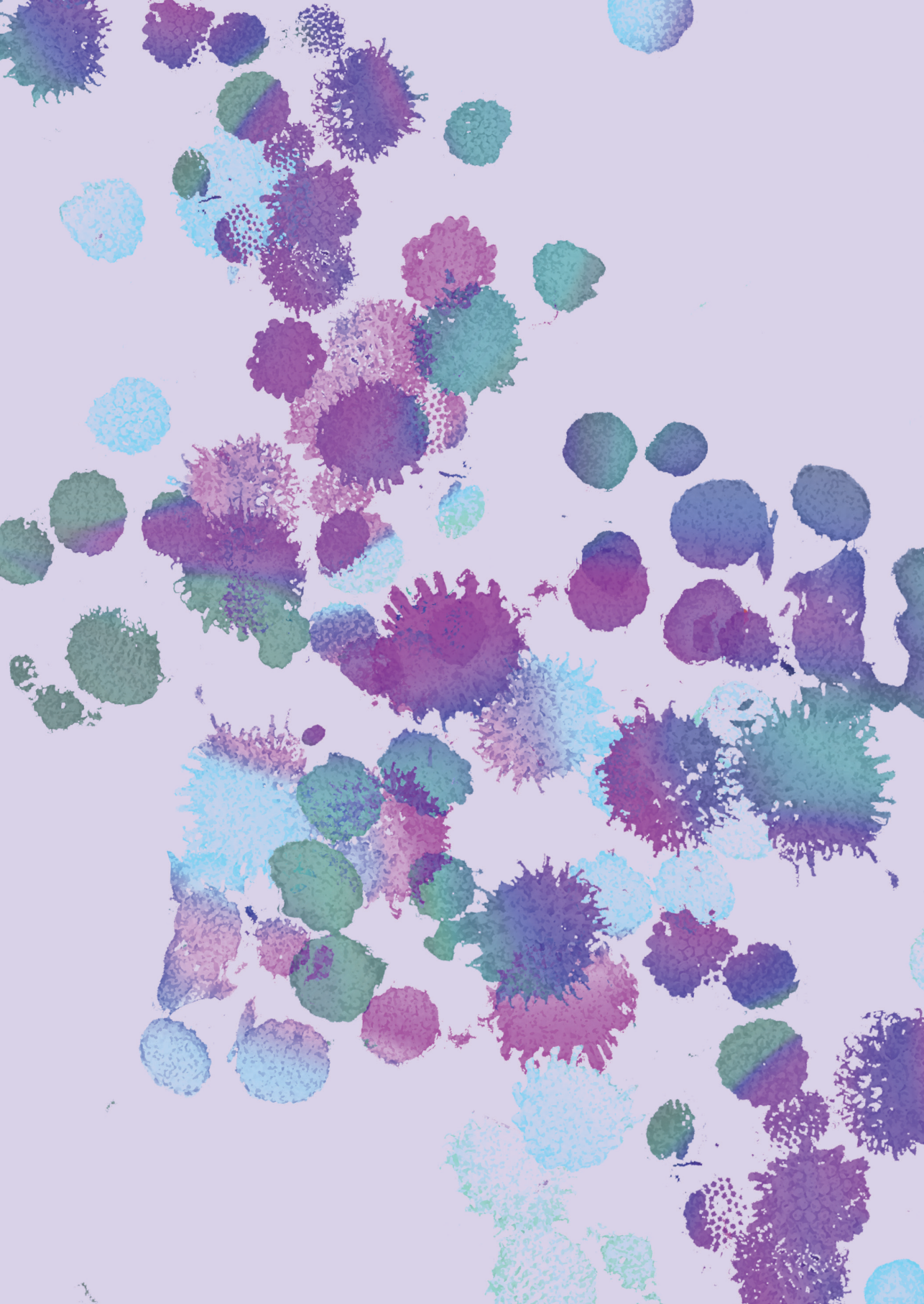
Pothast, C. R. (2026, February 12). *Primary T-cell responses against SARS-CoV-2 in patients with hematological disorders*. Retrieved from <https://hdl.handle.net/1887/4290106>

Version: Publisher's Version

[Licence agreement concerning inclusion of doctoral thesis in the Institutional Repository of the University of Leiden](#)

License: <https://hdl.handle.net/1887/4290106>

Note: To cite this publication please use the final published version (if applicable).



SARS-COV-2-SPECIFIC CD4⁺ AND CD8⁺ T CELL RESPONSES CAN ORIGINATE FROM CROSS-REACTIVE CMV-SPECIFIC T CELLS

Pothast, C. R., Dijkland, R. C., Thaler, M., Hagedoorn, R. S., Kester, M. G. D., Wouters, A. K., Hiemstra, P. S., van Hemert, M. J., Gras, S., Falkenburg, J. H. F., & Heemskerk, M. H. M.

(2022). *Elife*. DOI: 10.7554/eLife.82050

Chapter
2

ABSTRACT

Detection of SARS-coronavirus-2 (SARS-CoV-2) specific CD4⁺ and CD8⁺ T cells in SARS-CoV-2-unexposed donors has been explained by the presence of T cells primed by other coronaviruses. However, based on the relative high frequency and prevalence of cross-reactive T cells, we hypothesized CMV may induce these cross-reactive T cells. Stimulation of pre-pandemic cryo-preserved PBMCs with SARS-CoV-2 peptides revealed that frequencies of SARS-CoV-2-specific T cells were higher in CMV-seropositive donors. Characterization of these T cells demonstrated that membrane-specific CD4⁺ and spike-specific CD8⁺ T cells originate from cross-reactive CMV-specific T cells. Spike-specific CD8⁺ T cells recognize SARS-CoV-2 spike peptide FVSNGTHWF (FVS) and dissimilar CMV pp65 peptide IPSINVHHY (IPS) presented by HLA-B*35:01. These dual IPS/FVS-reactive CD8⁺ T cells were found in multiple donors as well as severe COVID-19 patients and shared a common T cell receptor (TCR), illustrating that IPS/FVS-cross-reactivity is caused by a public TCR. In conclusion, CMV-specific T cells cross-react with SARS-CoV-2, despite low sequence homology between the two viruses, and may contribute to the pre-existing immunity against SARS-CoV-2.

INTRODUCTION

The effectiveness of the innate and adaptive immune system is an important factor for disease outcome during infection with severe acute respiratory syndrome coronavirus 2 (SARS-CoV-2)¹. CD4⁺ and CD8⁺ T cells are important components of the adaptive immune system as CD4⁺ T cells promote antibody production by B cells and help cytotoxic CD8⁺ T cells to mediate cytotoxic lysis of SARS-CoV-2 infected cells². Whilst immunity is commonly measured solely based on antibody titers, research into coronavirus disease (COVID-19) pathophysiology and vaccination effectiveness has associated an effective T cell response with less severe COVID-19²⁻⁸. Additionally, SARS-CoV-2-specific T cell responses have been shown to be present in most individuals 6 months after infection or vaccination and remain largely unaffected by emerging variants of concern, illustrating their importance in generating durable immune responses⁹⁻¹⁷.

2

Besides *de novo* SARS-CoV-2-specific T cell responses in infected individuals, SARS-CoV-2-specific T cells have also been identified in unexposed individuals¹⁸⁻²². This finding indicates that T cells which were initially primed against other pathogens are able to cross-recognize SARS-CoV-2 antigen. This phenomenon is called heterologous immunity and can often be explained by genomic sequence homology between pathogens. Highly homologous DNA sequences are translated into similar proteins which can be processed and presented as epitopes with high sequence similarity in human leukocyte antigen (HLA). For this reason, most research has focused on cross-reactive T cells that are potentially primed by other human coronaviruses (HCoVs) since they share around 30% amino acid sequence homology with SARS-CoV-2²¹⁻²⁷. However, it has been postulated that SARS-CoV-2-specific T cells in unexposed individuals could also conceivably be primed by other, non-HCoVs^{22,28-30}. Furthermore, previous studies, although limited, have demonstrated the occurrence of cross-reactivity between two epitopes with relatively low sequence homology³¹⁻³⁶. This form of heterologous immunity is poorly understood and, therefore, predicting such cross-reactivity remains a challenge³⁷.

Pre-pandemic SARS-CoV-2-specific T cells are reportedly present in a relatively high proportion of the population, independent of geographical location, indicating that a highly prevalent pathogen could be the initial trigger of these cross-reactive T cells^{5,18-23,38}. Furthermore, these cross-reactive T cells should be present in relatively high frequencies, as they are detectable in antigen-induced stimulation assays without additional amplification steps^{5,18,19,22,23}. Cytomegalovirus (CMV) is a highly prevalent pathogen and usually induces high T cell frequencies, making CMV a potential trigger

for cross-reactive SARS-CoV-2-specific T cells ^{39,40}. This is supported by the finding that SARS-CoV-2 cross-reactive CD8⁺ T cells were increased in CMV-seropositive (CMV⁺) donors, and that previous CMV infection has been associated with severe COVID-19 ⁴¹⁻⁴³. Studies so far indicate that cross-reactive T cells can play a role in COVID-19 immunity but whether they are protective or pathogenic is unclear ^{24,26}. Taken together, we hypothesized that cross-reactive SARS-CoV-2-specific T cells might originate from the CMV-specific memory population.

In the present study, we aimed to identify SARS-CoV-2-specific cross-reactive CD4⁺ and CD8⁺ T cells in SARS-CoV-2-unexposed individuals. We found an increased presence of cross-reactive T cells in CMV⁺ donors and upon isolation and clonal expansion of the spike-reactive CD8⁺ and membrane-reactive CD4⁺ T cells we confirmed that these T cells were reactive against both SARS-CoV-2 and CMV. Interestingly, isolated CD8⁺ T cells recognizing a previously described CMV epitope IPSINVHHY presented by HLA-B*35:01 were cross-reactive with dissimilar SARS-CoV-2 spike peptide FVSNGTHWF presented by HLA-B*35:01, demonstrating that cross-reactivity does not solely depend on peptide sequence homology. The T cell receptor (TCR) isolated from these CD8⁺ T cells was found in multiple donors showing that pre-pandemic spike-reactive CD8⁺ T cells can be caused by a public CMV-specific TCR. Based on the reduced activation status compared to other SARS-CoV-2 specific T cells in severe COVID-19 patients, we hypothesize that these cross-reactive T cells are not important for clearing the virus at this late stage of the disease. However, these cross-reactive CD8⁺ T cells were shown to reduce spreading of SARS-CoV-2 infection *in vitro*, and in 2 out of 2 CMV⁺ severe COVID-19 patients these cross-reactive T cells were detected. This indicates that early in infection at the stage that no SARS-CoV-2 specific T cells are present yet, these cross-reactive T cells may play a role in preventing SARS-CoV-2 infection or reducing the severity of COVID-19.

RESULTS

SARS-CoV-2-specific T cell responses in SARS-CoV-2-unexposed PBMCs correlate with CMV seropositivity

To investigate whether SARS-CoV-2-specific CD4⁺ and CD8⁺ T cell responses in SARS-CoV-2-unexposed donors correlate with previous CMV infection, pre-pandemic cryopreserved PBMCs from CMV seropositive (CMV⁺, N=28) and CMV seronegative (CMV⁻, N=39) healthy individuals were stimulated overnight using SARS-CoV-2 15-mer peptide pools. These pools included 3 spike peptide pools that together overlap the entire spike gene (S, S1 and S+), membrane (M) and nucleocapsid (N) antigens from

SARS-CoV-2. To confirm that CMV⁺ individuals have CMV-specific T cells, reactivity against the most immunogenic CMV antigen, pp65, was also tested. Memory SARS-CoV-2-specific CD4⁺ T cells were characterized as CD154⁺CD137⁺ and memory SARS-CoV-2-specific CD8⁺ T cells were identified based on expression of CD137 and IFN- γ (**Figure 1A-B** and **Figure 1 – figure supplement 1**). As expected, all CMV⁺ donors displayed a CD4⁺ and/or CD8⁺ T cell response upon stimulation with pp65 (**Figure 1C-E**). No marked increase of CD4⁺ T cell responses were observed after SARS-CoV-2 spike and nucleocapsid stimulation in the CMV⁺ group compared to CMV⁻. However, 6 donors in the CMV⁺ group displayed a CD4⁺ T cell response against the membrane peptide pool which was not observed in the CMV⁻ group (**Figure 1C**). Furthermore, CD4⁺ T cell response against the membrane pool was accompanied by a CD4⁺ T cell response against pp65 (**Figure 1D**). In addition, CD8⁺ T cell responses were detected against spike peptides in two CMV⁺ donors which were not detected in CMV⁻ donors (**Figure 1E**). Interestingly, donors with a high CD8⁺ T cell response against SARS-CoV-2 spike peptides additionally displayed strong reactivity against pp65 (**Figure 1F**). Taken together, these results show that SARS-CoV-2-unexposed CMV⁺, but not CMV⁻, individuals had detectable CD4⁺ T cell responses against membrane peptides and CD8⁺ T cells targeting spike peptides. These SARS-CoV-2 responses were accompanied by T cell responses against pp65 and thus may indicate that SARS-CoV-2 T cell responses in pre-pandemic samples potentially are memory T cells targeting pp65.

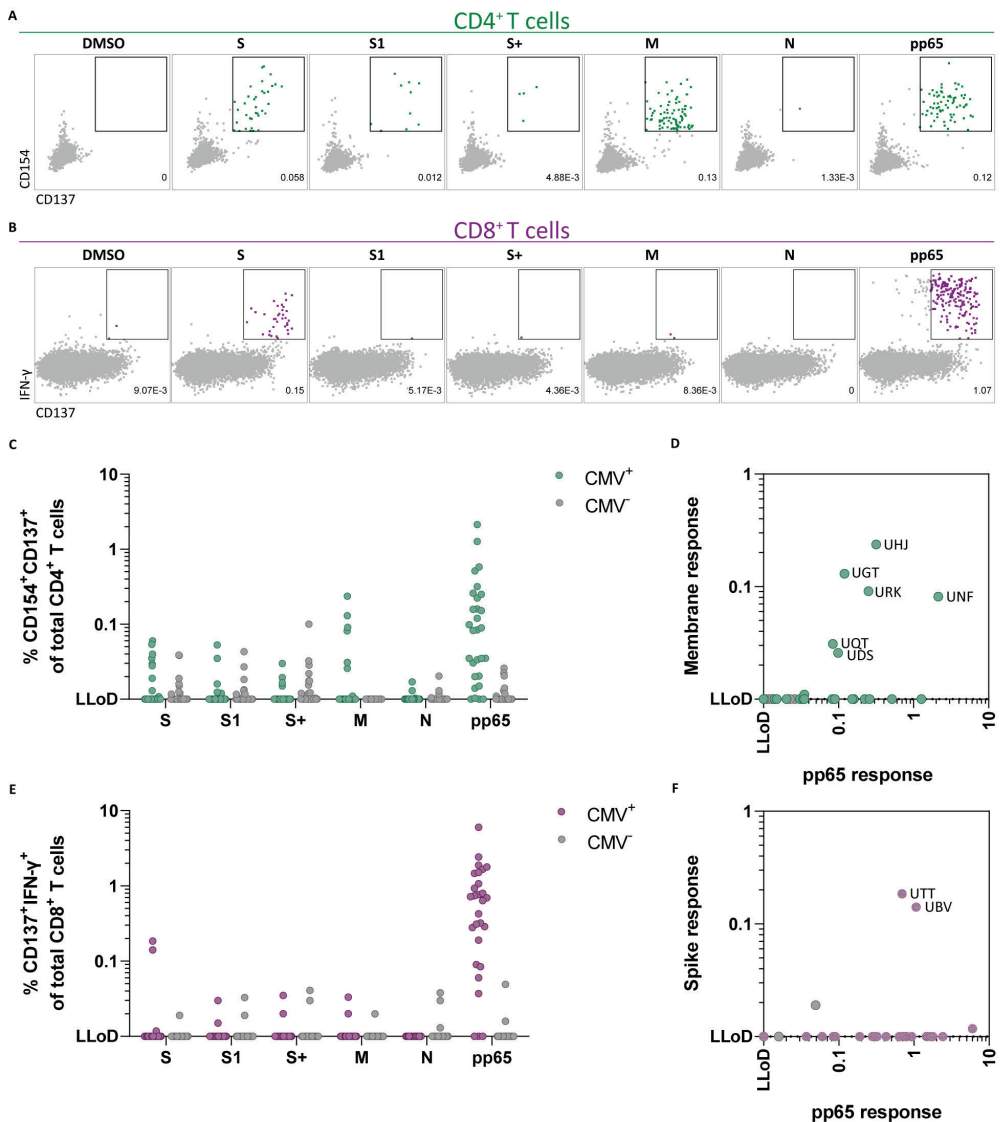


Figure 1 *Ex vivo* SARS-CoV-2-specific CD4⁺ and CD8⁺ T-cell responses in CMV-positive and -negative unexposed donors

Pre-pandemic cryo-preserved PBMCs were stimulated using SARS-CoV-2 spike (S, S1 and S+), membrane (M), nucleocapsid (N) and CMV pp65 peptide pools or not stimulated (DMSO). A) A representative flow cytometry example of a CD4⁺ T cell response in a SARS-CoV-2-unexposed donor. Numbers in plot represent frequencies of CD137⁺CD154⁺ cells of total CD4⁺ T cells. B) A representative flow cytometry example of a CD8⁺ T cell response in a SARS-CoV-2-unexposed donor. Numbers in plot represent frequencies of CD137⁺IFN- γ ⁺ cells of total CD8⁺ T cells. C) Scatter plot showing frequencies of CD137⁺CD154⁺ cells of total CD4⁺ T cells of CMV⁺ (green, N=28) and CMV⁻ (grey, N=39) donors. D) Frequencies of CD137⁺CD154⁺ cells of total CD4⁺ T cells in the membrane-stimulated condition (membrane response) plotted against pp65-stimulated condition (pp65 response). 3 letter codes

are anonymized codes of CMV⁺ (green) and CMV⁻ (grey) donors. E) Scatter plot showing frequencies of CD137⁺ IFN- γ ⁺ cells of total CD8⁺ T cells of CMV⁺ (green, N=28) and CMV⁻ (grey, N=39) donors. F) Frequencies of CD137⁺IFN- γ ⁺ cells of total CD8⁺ T cells in the spike-stimulated condition (spike response) plotted against pp65-stimulated condition (pp65 response).

Pre-pandemic SARS-CoV-2-specific CD4⁺ and CD8⁺ T cells recognize pp65 peptides from CMV

To confirm that pre-pandemic SARS-CoV-2-specific T cells are able to recognize peptides from pp65, these SARS-CoV-2-specific T cells were isolated and clonally expanded. SARS-CoV-2-unexposed (pre-pandemic cryopreserved) PBMCs from a CMV⁺ individual showing a CD4⁺ T cell response against SARS-CoV-2 membrane protein (donor UGT) were stimulated with the membrane peptide pool and single cell sorted based on CD137 upregulation (**Figure 2 – figure supplement 1**). After clonal expansion, 20 out of 27 screened T cell clones produced IFN- γ when stimulated with membrane peptide pool compared to no peptide stimulation (data not shown). T cell clones 4UGT5, 4UGT8 and 4UGT17, all three expressing a different TCR, were used for further experiments (**Figure 2 – figure supplement 2A**). As hypothesized, the T cell clones were reactive against both SARS-CoV-2 membrane antigen and CMV pp65 when loaded on HLA-matched Epstein-Barr virus lymphoblastoid cell lines (EBV-LCLs) (**Figure 2A**). Interestingly, IFN- γ production by the T cell clones was significantly increased when stimulated with pp65 peptides compared to membrane peptides indicating higher avidity for CMV compared to SARS-CoV-2 (**Figure 2B**). To identify which peptide in pp65 is recognized, reactivity of T cell clone 4UGT8 against a pp65 library was measured which resulted in recognition of three sub pools which contained peptide AGILARNLVP (Figure 2 – **figure supplement 2B-C**). HLA-mismatched EBV-LCLs were retrovirally transduced with HLA Class II molecules that were commonly shared between donors that had a detectable CD4⁺ T cell response against the membrane and pp65 peptide pool (**Figure 1D**). T cell clone 4UGT8 recognized both peptide pools and the AGI peptide only when presented in HLA-DRB3*02:02 (**Figure 2C and figure 2 – figure supplement 2D**). The SARS-CoV-2 membrane protein epitope recognized by these cross-reactive T cells remains unidentified as *in vitro* experiments and *in silico* prediction methods failed to identify the epitope. A similar approach was applied for CD8⁺ T cells in which T cell clones were generated after SARS-CoV-2 spike peptide pool stimulation of PBMCs from CMV⁺ donor UTT (**Figure 2 – figure supplement 1**). The isolated CD8⁺ T cell clones were screened for their reactivity with SARS-CoV-2 spike which showed that 23 out of the 28 T cell clones produced IFN- γ upon spike peptide pool stimulation (data not shown). TCR sequencing revealed that all 23 T cell clones expressed the same TCR (**Figure 2 – figure supplement 3A**). T cell clone 8UTT6 was selected for further testing and analyzed for its cross-reactivity towards SARS-CoV-2 spike and CMV pp65 peptide pools. Additionally, the HLA restriction of T cell clone 8UTT6 was hypothesized to be HLA-B*35:01 as the

unexposed donors with a CD8⁺ T cell response against SARS-CoV-2 spike (UTT and UVB) both expressed HLA-B*35:01. The results confirmed that T cell clone 8UTT6 recognized spike as well as pp65 peptide pool presented by K562 cells transduced with HLA-B*35:01 but not transduced with HLA-A*11:01 (**Figure 2D**). To identify the spike epitope, reactivity of clone 8UTT6 against the 15-mer spike peptide library was measured. For the identification of the CMV epitope, an unbiased approach was performed using the nonamer combinatorial peptide library (CPL) assay. Recognition patterns were analyzed using netMHC 4.0 analysis for predicted binding to HLA-B*35:01, which revealed SARS-CoV-2 spike peptide FVSNGTHWF (FVS, S₁₀₉₄₋₁₁₀₃) and CMV pp65 IPSINVHHY (IPS, pp65₁₁₂₋₁₂₁) as the most likely epitopes (**Figure 2 – figure supplement 3B-E**). The FVS and IPS peptides were indeed recognized by clone 8UTT6 (**Figure 2E**). Importantly, the IPS peptide was recognized with higher avidity compared to the FVS peptide by clone 8UTT6 (**Figure 2F**). Supporting these findings, the same TCR β chain was already described and demonstrated to be specific for IPS in HLA-B*35:01 ⁴⁴. Taken together, SARS-CoV-2 reactive CD4⁺ and CD8⁺ T cells in pre-pandemic samples cross-reacted with CMV and SARS-CoV-2 peptides.

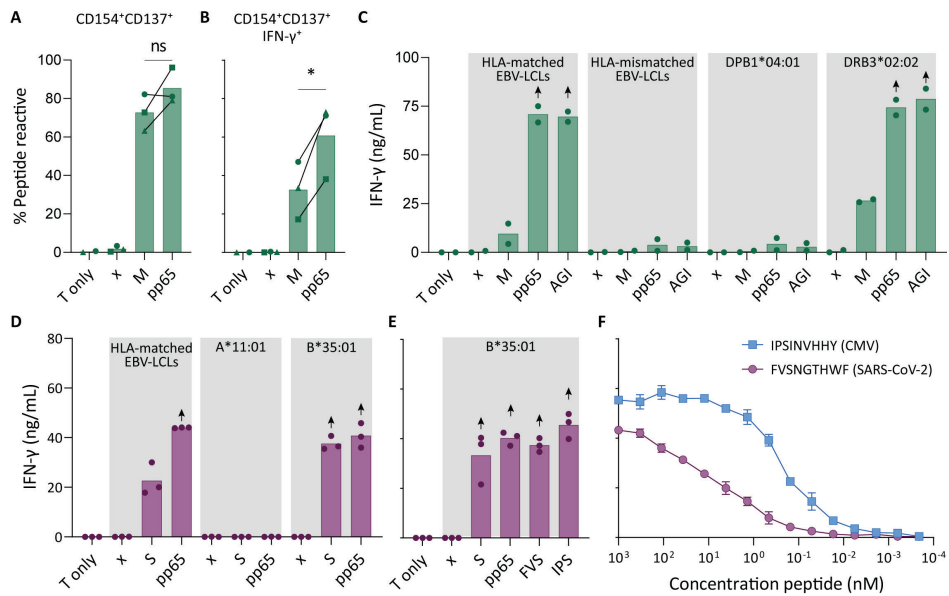


Figure 2 Recognition of SARS-CoV-2 and CMV by pre-existing CD4⁺ and CD8⁺ T cells

Clonally expanded CD4⁺ T cells from donor UGT and CD8⁺ T cells from donor UTT were overnight co-cultured with peptide-pulsed stimulator cells. A-B) Percentages of CD154⁺, CD137⁺ and/or IFN- γ ⁺ cells of cross-reactive CD4⁺ T cell clones after overnight culture (T only) or after overnight co-culture with HLA-matched EBV-LCLs that were not peptide pulsed (x) or loaded with membrane (M) or pp65 peptide pool, measured by flow cytometry. Dots represent the mean of experimental repeats of 4UGT5 (square, 1 repeat), 4UGT8 (circles, 4 repeats) and 4UGT17 (triangle, 2 repeats). Significance was tested by a paired *t*-test. C) Bar graphs showing ELISA measurement of secreted IFN- γ after co-culturing of a representative clone, 4UGT8 clone, with HLA-matched or HLA-mismatched EBV-LCLs. HLA-mismatched EBV-LCLs were retrovirally transduced with HLA class II molecule as depicted in figure. Stimulator cells were peptide-pulsed with membrane (M) peptide pool, pp65 peptide pool or AGILARNLVP (AGI) peptide. Data points are experimental duplicates. Black arrows indicate that values were above plateau value of the ELISA calibration curve. D-E) Bar graphs showing ELISA measurement of secreted IFN- γ after co-culturing of a representative clone, 8UTT6 clone, with HLA-matched EBV-LCLs or K562s transduced with HLA-B*35:01 or HLA-A*11:01. Stimulator cells were peptide-pulsed with spike (S) peptide pool, pp65 peptide pool, IPSINVHHY (IPS) peptide or FVSNGTHWF (FVS) peptide. Data points are technical triplicates. F) Peptide titration of IPS peptide (blue) and FVS peptide (purple) in a co-culture assay with 8UTT6 clone.

Similarity at the C-terminal part of the peptides could drive T cell cross-reactivity

To understand the molecular basis of T cell cross-reactivity between dissimilar peptides FVS and IPS, we modelled the FVS structure based on the solved structure of the IPS peptide bound to HLA-B*35:01 (Figure 3) ⁴⁵. The two peptides share 2 residues (P3-S and P7-H) and have 2 similar residues (P6-T/V and P9-F/Y) based on similar biochemical properties and size. Residue substitutions from the IPS to FVS peptide were possible without major steric clashes with the HLA or peptide residues. The lack of secondary anchor residue at position 5 in the FVS peptide (P5-N/G) might change the conformation of the central part of the peptide, that could be similar to the

one observed in the spike-derived peptide IPF (S₈₉₆₋₉₀₄) in complex with HLA-B*35:01 (**Figure 3 – figure supplement 1**)⁴⁶. The primary anchor in the FVS peptide are P2-V and P9-F, both within the favored residues at those positions for HLA-B35-restricted peptide⁴⁷. Overall, the FVS peptide might adopt a similar backbone conformation compared to the IPS peptide, which would place in both peptides a small hydrophobic residue at position 6 (P6-T/V), a histidine at position 7, and a residue with a large side-chain at position 8 (P8-W/H).

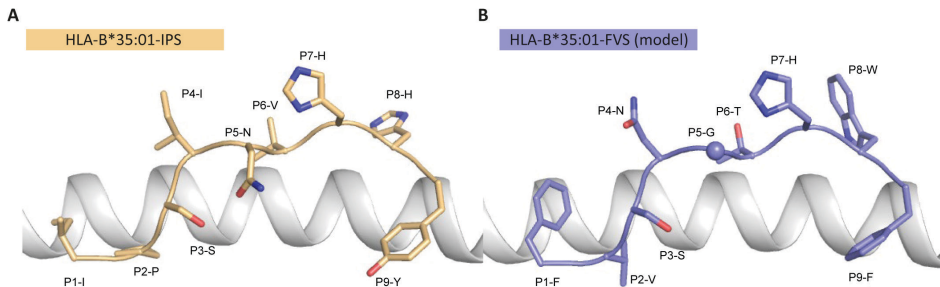


Figure 3 Model of the HLA-B*35:01-FVS structure

A) Crystal structure of the HLA-B*35:01-IPS complex with the HLA in white cartoon and the IPS peptide in clear orange cartoon and stick. B) Model of the HLA-B*35:01-FVS complex with the HLA in white cartoon and the FVS peptide in blue cartoon and stick. The sphere represents the C α atom of the FVS peptide P5-G residue.

IPS/FVS-specific cross-reactive CD8 $^{+}$ T cells are detectable in multiple individuals

To investigate the prevalence and phenotype of IPS/FVS cross-reactive T cells, HLA-B*35:01 $^{+}$ CMV $^{+}$ healthy donors were screened for IPS/FVS-specific T cells using tetramers consisting of HLA-B*35:01-FVS (B*35/FVS-tetramer) and HLA-B*35:01-IPS (B*35/IPS-tetramer) (**Figure 4 - figure supplement 1**). Tetramer staining of PBMCs from donor UTT demonstrated that not all T cells that bound to B*35/IPS-tetramer were able to bind to the B*35/FVS-tetramer as well. However, all T cells that bound to B*35/FVS-tetramer were also binding to the B*35/IPS-tetramer (**Figure 4A**). This observation indicates that IPS/FVS cross-reactivity is dictated by specific TCR sequences which was further supported by the lack of binding to B*35/FVS-tetramer by an IPS-specific T cell clone with a different TCR (**Figure 4B**). Screening of SARS-CoV-2-unexposed, CMV $^{+}$ and HLA-B*35:01 donors (N=37) showed that nearly all CMV $^{+}$ donors had IPS-specific T cells with frequencies above background level and, interestingly, three of the analyzed donors (UTT, UVB and SFW) presented with clearly detectable IPS/FVS-specific T cells (**Figure 4C**). Furthermore, IPS/FVS-specific T cells displayed an effector memory phenotype (CCR7/CD45RA), confirming a memory repertoire origin and, interestingly, a less differentiated phenotype compared to IPS-specific T cells (**Figure 4D**). In summary, IPS/FVS cross-reactivity is dependent on the TCR clonotype and these cross-reactive T cells are detected in multiple donors.

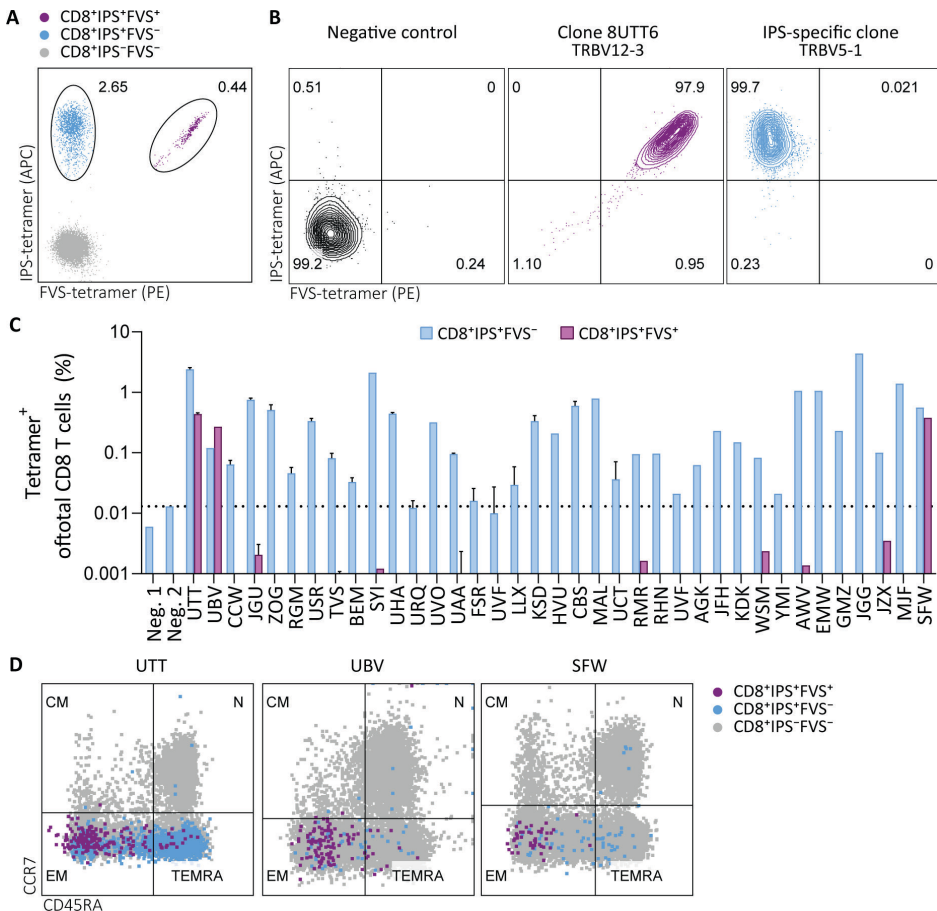


Figure 4 Tetramer detection of IPS/FVS-specific CD8⁺ T cells in CMV⁺ and HLA-B*35:01⁺ donors

Flow cytometry measurement of PBMCs or T cell clones that are binding to B*35/IPS-tetramer (blue), B*35/FVS-tetramer (purple) or to neither (grey). A) Flow cytometry dot plot showing percentages of tetramer-binding cells of total CD8⁺ T cells in PBMCs from donor UTT. B) Dot plot showing percentages of tetramer-binding of 8UTT6 clone and an IPS-specific clone with their IMGT variable region of T cell receptor β -chain (TRBV) depicted. As a negative control (neg. ctrl.), a T cell clone recognizing a non-relevant peptide in HLA-B*35:01 was included. C) Bar graph showing frequencies of tetramer-binding of total CD8⁺ from PBMCs of healthy CMV⁺ and HLA-B*35:01⁺ donors. Error bars represent standard deviation of experimental duplicates. Dotted line represents background level which was based on HLA-B*35:01⁺ donors (neg.). D) Dot plot showing expression of CCR7 and CD45RA by total CD8⁺ T cells and tetramer-binding T cells in PBMCs from UTT, UBV and SFW. Quadrants separates differentiation subsets into naïve (N), central memory (CM), effector memory (EM) and terminally differentiated effector memory (TEMRA).

IPS/FVS cross-reactivity is underpinned by a public TCR

To investigate whether the IPS/FVS-specific CD8⁺ T cells found in multiple donors expressed a similar TCR, B*35/FVS-tetramer-binding T cells were isolated and the

TCR α and β chains sequenced (**Figure 5 - figure supplement 1**). Sequencing was performed for samples with clear detection of IPS/FVS-specific T cells (UTT, UVB, SFV) and one donor with detectable, but below the limit of accurate detection of B*35/FVS-tetramer $^+$ T cells (JZX) (**Figure 4C**). Interestingly, B*35/FVS-isolated T cells from all donors displayed amino acid identical dominant complementary-determining region 3 (CDR3) of the α -chain, CAGNQGGKLIF (CDR3 α ^{CAGNQG}), and β -chain, CASSLALDEQFF (CDR3 β ^{CASSLA}) (**Figure 5A**). This observation thereby shows that IPS/FVS cross-reactivity is caused by a public TCR. These identical CDR3s were not a result of sequencing artefact as nucleotide alignment revealed minor differences between samples (**Figure 5 – figure supplement 2**). In addition to B*35/FVS-isolated T cells, T cells that bound B*35/IPS-tetramer were isolated and sequenced in parallel. Both CDR3 α ^{CAGNQG} and CDR3 β ^{CASSLA} were identified in all samples and shown to be among the most dominant TCRs. Remarkably, this was also observed in donor JZX which showed IPS/FVS-tetramer $^+$ T cells below background level, indicating that in more than 3 out of 37 donors this public TCR is present. (**Figure 5C**). Taken together, IPS/FVS-specific T cells express an identical TCR, found in multiple donors, indicating that public TCRs can exhibit cross-reactive properties.

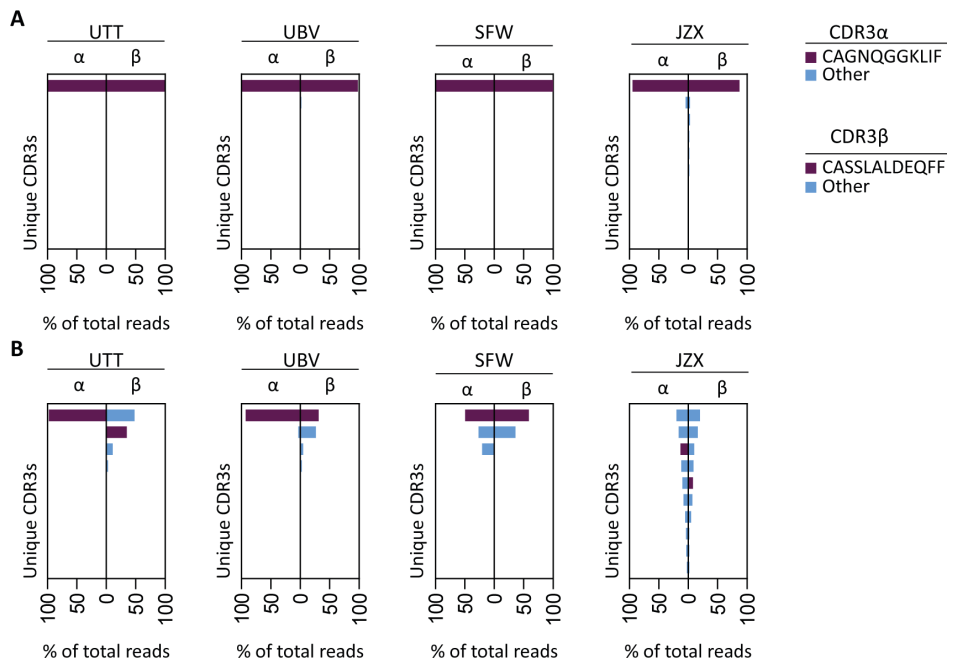


Figure 5 TCR sequencing of IPS/FVS-specific T cells

PBMCs from healthy CMV⁺ and HLA-B*35:01⁺ donors were sorted on B*35/IPS- or B*35/FVS-tetramer binding and directly sequenced for their TCR alpha and beta chain. Unique CDR3 sequences are depicted in two-sided bar graphs in which the left side shows abundance of CDR3 sequences from the TCR α-chain (CDR3α) and the right side shows abundance of CDR3 sequences from the TCR β-chain (CDR3β). Bar graphs are purple if the CDR3α has the CAGNQGGKLIF sequence or the CDR3β has the CASSLALDEQFF sequence, all other found sequences are depicted in blue. CDR3s with less than 1% abundance were excluded from the figure. A) Two-sided bar graphs showing abundances of unique CDR3 sequences of samples sorted on binding to B*35/FVS-tetramer. B) Two-sided bar graphs showing abundances of unique CDR3 sequences of samples sorted on binding to B*35/IPS-tetramer.

IPS/FVS cross-reactive CD8⁺ T cells are able to recognize SARS-CoV-2 infected cells but do not show an activated phenotype during acute disease

To investigate whether IPS/FVS-specific CD8⁺ T cells can play a role during SARS-CoV-2 infection, the function of IPS/FVS-specific T cells in an *in vitro* model and the activation state of these T cells during acute SARS-CoV-2 infection in severe COVID-19 patients was assessed. Firstly, the reactivity of IPS/FVS-specific T cells against K562 transduced with the spike gene was measured which showed that the T cells were able to recognize endogenously processed and presented peptide (Figure 6A). To investigate whether the IPS/FVS-specific T cells can recognize SARS-CoV-2-infected cells and thereby limit viral spread, Calu-3 airway epithelial cells were infected with live SARS-CoV-2 virus (wildtype) and incubated for 6 hours before co-culturing with CD8⁺ T cells. SARS-CoV-2 spike-specific CD8⁺ T cells from a SARS-CoV-2 vaccinated donor were able to reduce intracellular SARS-CoV-2 RNA copies at both 0.05 and 0.5

multiplicity of infection (MOI) 24 hours post infection (**Figure 6B-C**). Interestingly, IPS/FVS-specific CD8⁺ T cells were able to reduce SARS-CoV-2 intracellular RNA copies in Calu-3 cells infected with 0.05 MOI (MOI (**Figure 6B**). Incubating with 10-fold more virus (0.5 MOI) resulted in no difference in RNA copies compared to the no T cell control (**Figure 6C**). To further investigate the function of IPS/FVS-specific CD8⁺ T cells *ex vivo*, the activation state of these T cells was evaluated during severe COVID-19 disease in two CMV⁺ HLA-B*35:01⁺ patients. The activation state was measured by expression of activation markers CD38 and HLA-DR as these markers are highly expressed on SARS-CoV-2-specific CD8⁺ T cells during severe COVID-19 (**Figure 6D**)⁵. Interestingly, IPS/FVS-cross-reactive T cells were detected in 2 out of 2 CMV⁺ HLA-B*35:01⁺ patients suffering from severe COVID-19, whereas the cross-reactive T cells were detected in 3 out of 37 healthy CMV⁺ HLA-B*35:01⁺ donors (**Figure 4C and 6E**). The expression of CD38 and HLA-DR was lower compared to the SARS-CoV-2-specific CD8⁺ T cells and not considerably increased compared to IPS-specific T cells that were not cross-reactive with FVS (**Figure 6D-E**). These results indicate that IPS/FVS-specific CD8⁺ T cells recognize SARS-CoV-2-infected cells and are able to limit SARS-CoV-2 replication at low virus titers. However, IPS/FVS-specific T cells did not show an activated phenotype during acute severe SARS-CoV-2 infection.

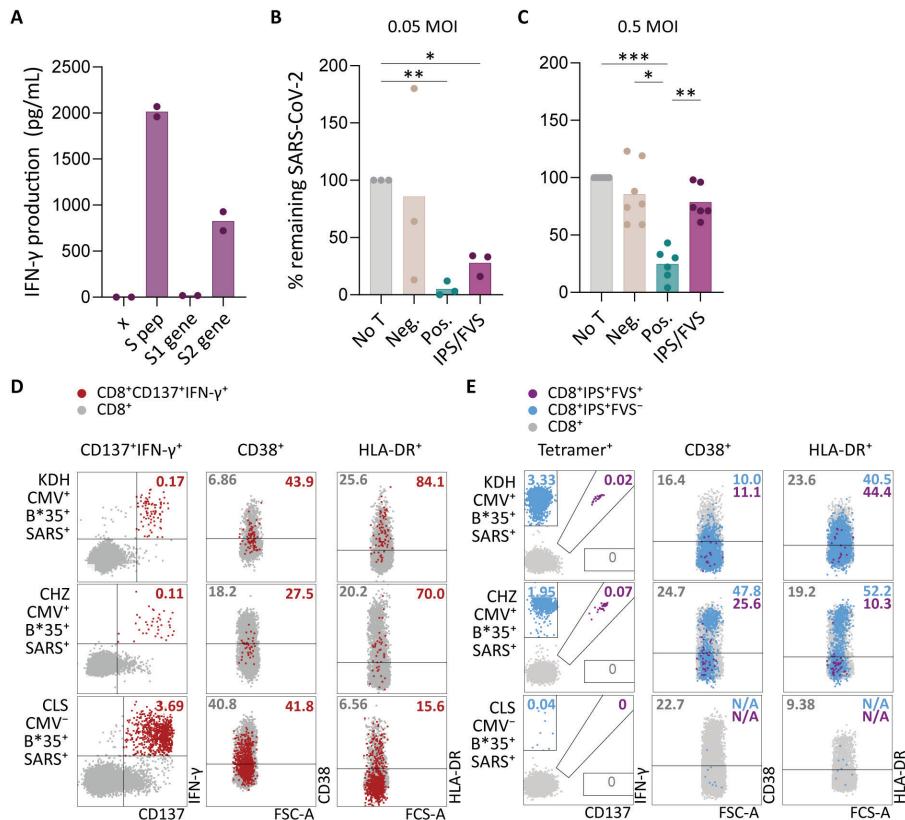


Figure 6 Ex vivo and in vitro evaluation of IPS/FVS-specific T cells

A) IFN- γ release of IPS/FVS-specific CD8⁺ T cells after co-incubation with K562 that were untransduced (x), loaded with spike peptide pool (S pep), or transduced with nucleotide 1 to 2082 (S1 gene) or nucleotide 2052 to 3822 (S2 gene) of the spike gene. B-C) Calu-3 cells were transduced to express HLA-B*35:01 and infected with the wildtype SARS-CoV-2 virus. 6 hours post infection, IPS/FVS-specific CD8⁺ T cells were added in a 10:1 effector to target ratio. SARS-CoV-2 spike-specific T cells, isolated from COVID-19 vaccinated individuals, that recognize VASQSIAY presented in HLA-B*35:01 or YLQPRTEFL presented in HLA-A*02:01 functioned as a positive control (pos.) or negative control (neg.), respectively. Cells were harvested 24 hpi to measure intracellular viral RNA. Bar graphs show the means of percentage reduction in SARS-CoV-2 intracellular RNA copies compared to the no T cell condition (no T) as measured by RT-qPCR, at 24 hpi post infection using a MOI of 0.05 or 0.5. One-way ANOVA was applied test statistical differences between conditions and only comparisons with $p < 0.05$ are shown. (D-E) Flow cytometry analysis of CD38 and HLA-DR expression on CD8⁺ T cells in PBMCs from severe COVID-19 patients that were CD137⁺IFN- γ after SARS-CoV-2 nucleocapsid peptide stimulation (red), only bound to B*35/IPS-tetramer (blue) or bound to both B*35/IPS- and B*35/FVS-tetramer (purple). All other CD8⁺ T cells are grey. Two patients were HLA-B*35:01⁺CMV⁺ (KDH and CHZ) and, as a control, one patient was HLA-B*35:01⁺CMV⁻ (CLS). Detection of B*35/IPS- and B*35/FVS-specific T cells and expression of the activation markers were measured and compared within the same sample.

DISCUSSION

SARS-CoV-2-specific T cells in pre-pandemic cryo-preserved samples have been reported in several studies. The majority of these studies describe T cell immunity against other HCoVs as the main source of these T cells²¹⁻²⁷. However, some studies have postulated that pre-pandemic SARS-CoV-2-specific T cells could be derived from other sources^{22,28-30}. Our findings demonstrate that CMV pp65-specific CD4⁺ T cells cross-react with the membrane protein from SARS-CoV-2 and CMV pp65-specific CD8⁺ T cells are able to cross-react with SARS-CoV-2 spike protein. The cross-reactive CD8⁺ T cells recognized known CMV epitope IPSINVHHY in HLA-B*35:01 and cross-reacted with the SARS-CoV-2 epitope FVSNGTHWF in HLA-B*35:01. These IPS/FVS-specific CD8⁺ T cells were detected in multiple donors all expressing an identical T cell receptor, indicating that cross-reactivity with SARS-CoV-2 can be caused by a CMV-specific public TCR. Functional and phenotypic assessment of the IPS/FVS-specific CD8⁺ T cells indicated their capacity to reduce low concentrations of SARS-CoV-2 *in vitro* but these cross-reactive T cells detected in two severe COVID-19 patients were not activated based on phenotypic characterization.

To our knowledge this is the first study to identify CMV-specific T cells that are cross-reactive with SARS-CoV-2. The cross-reactive CD4⁺ T cells recognized CMV pp65 epitope AGILARNLVP in HLA-DRB3*02:02 and were able to cross-react with an as of yet unidentified, SARS-CoV-2 membrane epitope in HLA-DRB3*02:02.⁴² Previous studies have reported the presence of membrane-specific CD4⁺ T cell responses in SARS-CoV-2-unexposed donors utilizing the same commercially available membrane peptide pool, yet these studies did not aim to identify the peptide-HLA restriction^{5,26}. AGI-specific CD4⁺ T cells have been described to be cross-reactive towards SARS-CoV-2 spike which is in contrast to our finding⁴². The cross-reactive CD8⁺ T cells recognize the CMV epitope IPSINVHHY and SARS-CoV-2 epitope FVSNGTHWF presented in HLA-B*35:01. IPS/FVS-specific T cells were possibly detected previously but never further investigated or characterized^{48,49}. Both cross-reactive CD4⁺ and CD8⁺ T cells displayed a higher avidity for the CMV epitope compared to the epitope derived from SARS-CoV-2. In contrast, other studies have reported an equal or even higher avidity for the SARS-CoV-2 epitope compared to the epitopes derived from the HCoV for which the T cells were hypothesized to be primed against^{21,23,27,50}. This appears to be contradictive since it has been shown that repeated exposure results in selection of high avidity T cell clonotypes which are able to clear viral infection and protect against reinfection⁵¹⁻⁵⁴. Cross-reactive T cells would therefore most likely display a higher avidity for the source pathogen compared to the avidity for SARS-CoV-2, as reported in this study. This discrepancy could be caused by the fact that previous

studies focused on other HCoVs since they share high sequence homology with SARS-CoV-2, thereby potentially missing the true source of these particular T cells²¹⁻²⁷. Alternatively, samples frozen down during the pandemic were considered unexposed if the donors displayed neither SARS-CoV-2-specific antibodies nor a history of COVID-19-like symptoms^{23,26,50}. However, SARS-CoV-2 infection does not necessarily lead to symptoms nor a detectable antibody response^{55,56}. The described reduced avidity for HCoV therefore could imply that these cross-reactive T cells were derived from the SARS-CoV-2-induced repertoire. Taken together, whereas cross-reactive T cells recognizing SARS-CoV-2 have been primarily described to be derived from other HCoVs, the contribution of these other HCoVs as initial primers of the T cell response may have been over-estimated due to experimental design. Further studies are required to identify other potential sources of cross-reactivity with low sequence homology yet high prevalences such as CMV, EBV, influenza or non-viral pathogens.

The identified cross-reactive CD8⁺ T cells appeared to recognize CMV peptide IPSINVHHY and a dissimilar peptide FVSNGTHWF derived from SARS-CoV-2. *Ex vivo* detected heterologous CD8⁺ T cell immunity against two pathogens caused by dissimilar epitopes presented in the same HLA is rarely reported^{31,36}. Nevertheless, ample studies have investigated the underlying mechanisms of such T cell-mediated cross-reactivity. Heterologous immunity can be caused by the expression of a dual TCR which means that two TCR α - or β -chains are expressed simultaneously, resulting in two distinctive TCRs within one T cell⁵⁷. However, here we identified a single TCR in cross-reactive T cells excluding this hypothesis. Recognition of two distinct epitopes by a single TCR can be explained by shape similarity once the peptides are bound to the HLA molecule, and this shape similarity, or molecular mimicry, can underpin T cell cross-reactivity⁵⁸. Possible other underlying mechanisms are reduced footprint of the TCR with peptide^{59,60}, an altered TCR-docking angle⁶¹, or plasticity of the peptide-MHC complex^{32,61} or TCR⁶². Here, similarity between the IPS and FVS peptides in backbone conformation and the C-terminal part might underpin the T cell cross-reactivity observed, as the majority of TCR docks preferentially towards the C-terminal of the peptide⁶³. Solving the crystal structure of the IPS/FVS-TCR binding to HLA-B*35:01-FVS and -IPS would be necessary to provide insight in the binding properties of the public TCR.

IPS/FVS-specific CD8⁺ T cells were able to reduce SARS-CoV-2 spread *in vitro* when exposed to a low virus concentration, which is supported by our finding that two out of two tested severe COVID-19 patients had clearly detectable IPS/FVS-specific CD8⁺ T cells while the prevalence in healthy donors was 3 out of 37. The presence of these cross-reactive memory T cells in circulation may be an advantage during

initial SARS-CoV-2 infection as rapid T cell responses were associated with less severe COVID-19 ^{2,7,25}. However, the cross-reactive CD8⁺ T cells were less efficient compared to SARS-CoV-2-specific, vaccination-primed T cells in limiting viral spread *in vitro* which can be explained by the reduced avidity of the cross-reactive T cells for the spike protein compared to CMV. This study also demonstrated that IPS/FVS-specific CD8⁺ T cells did not display the same degree of activation as observed for the SARS-CoV-2-specific T cells during severe COVID-19. Additionally, despite the presence of the cross-reactive CD8⁺ T cells, these individuals developed severe disease. These observations together indicate that IPS/FVS-specific CD8⁺ T cells might be able to reduce SARS-CoV-2 spread at initial infection, but likely do not play a significant role in the pathogenesis of severe COVID-19. One limitation is that our study focused on circulating T cells, and we cannot exclude the possibility that cross-reactive CD8⁺ T cells present in lung tissue did display an activated phenotype. Another limitation of this study is the small severe COVID-19 cohort that was investigated and literature describing the role of cross-reactive T cells is scarce ^{24,26}. In summary, additional studies using larger cohorts are required to fully elucidate the potential role of cross-reactive CD8⁺ T cells in disease.

In conclusion, pre-pandemic SARS-CoV-2-specific T cells can derive from non-homologous pathogens such as CMV. This expands the potential origin of these pre-pandemic SARS-CoV-2-specific CD4⁺ and CD8⁺ T cell beyond other HCoVs. The cross-reactive CD8⁺ T cells were reactive towards dissimilar epitopes and this cross-reactivity was caused by a public TCR, which has been rarely observed so far. Our data points towards a role of the cross-reactive T cells in reducing SARS-CoV-2 viral load in the early stages of infection, prior to priming of SARS-CoV-2 specific T cells. Altogether, these results aid in further understanding heterologous T cell immunity beyond common cold coronaviruses and facilitates the investigation into the potential role of cross-reactive T cells in COVID-19.

METHODS

Key Resourced Table

Key Resources Table				
Reagent type (species) or resource	Designation	Source or reference	Identifiers	Additional information
Peptide, recombinant protein	SARS-CoV-2 Spike (S), 15-mers, 11aa overlapping peptide pool	Miltenyi	130-126-701	1 µg/mL
Peptide, recombinant protein	SARS-CoV-2 Spike (S1), 15-mers, 11aa overlapping peptide pool	Miltenyi	130-127-041	1 µg/mL
Peptide, recombinant protein	SARS-CoV-2 Spike (S+), 15-mers, 11aa overlapping peptide pool	Miltenyi	130-127-312	1 µg/mL
Peptide, recombinant protein	SARS-CoV-2 Membrane (M), 15-mers, 11aa overlapping peptide pool	Miltenyi	130-126-703	1 µg/mL
Peptide, recombinant protein	SARS-CoV-2 Nucleocapsid (N), 15-mers, 11aa overlapping peptide pool	Miltenyi	130-126-699	1 µg/mL
Peptide, recombinant protein	CMV pp65, 15-mers, 11aa overlapping peptide pool	JPT	Custom-made	1 µg/mL
Peptide, recombinant protein	CMV pp65 peptide library, 15-mers, 11aa overlapping	JPT	Custom-made	1 µg/mL
Peptide, recombinant protein	SARS-CoV-2 Spike peptide library, 15-mers, 11aa overlapping	SB Peptides	SB043	1 µg/mL

Key Resourced Table *Continued*

Key Resources Table				
Reagent type (species) or resource	Designation	Source or reference	Identifiers	Additional information
Peptide, recombinant protein	CMV, VFTWPPWQAGILARN	LUMC	Custom-made	1 µg/mL
Peptide, recombinant protein	CMV, PPWQAGILARNLVPML	LUMC	Custom-made	1 µg/mL
Peptide, recombinant protein	CMV, AGILARNLVPMVATV	LUMC	Custom-made	1 µg/mL
Peptide, recombinant protein	CMV, ARNLVPMVATVQGQN	LUMC	Custom-made	1 µg/mL
Peptide, recombinant protein	CMV, VPMVATVQGQNLKYQ	LUMC	Custom-made	1 µg/mL
Peptide, recombinant protein	CMV, AQGDDDVWTSGSDSD	LUMC	Custom-made	1 µg/mL
Peptide, recombinant protein	CMV, SSACTSGVMTRGR	LUMC	Custom-made	1 µg/mL
Peptide, recombinant protein	CMV, PKRRRHRQDALPGPC	LUMC	Custom-made	1 µg/mL
Peptide, recombinant protein	SARS-CoV-2, FVSNGTHWF	LUMC	Custom-made	1 µg/mL
Peptide, recombinant protein	CMV, IPSINVHHY	LUMC	Custom-made	1 µg/mL
Antibody	rat monoclonal anti- human CCR7 (BV711)	BD Biosciences	Cat.#563712 RRID:AB_2738386	FC (1:100)
Antibody	mouse monoclonal anti-human CD137 (APC)	BD Biosciences	Cat.#550890 RRID:AB_398477	FC (1:75)

Key Resources Table				
Reagent type (species) or resource	Designation	Source or reference	Identifiers	Additional information
Antibody	mouse monoclonal anti-human CD14 (FITC)	BD Biosciences	Cat.#555397 RRID:AB_395798	FC (1:100)
Antibody	mouse monoclonal anti-human CD154 (Pacific Blue)	Biolegend	Cat.#310820 RRID:AB_830699	FC (1:300)
Antibody	mouse monoclonal anti-human CD19 (FITC)	BD Biosciences	Cat.#555412 RRID:AB_395812	FC (1:100)
Antibody	mouse monoclonal anti-human CD4 (PE-Cy7)	Beckham Coulter	Cat.#737660 RRID:AB_2922769	FC (1:300)
Antibody	mouse monoclonal anti-human CD4 (FITC)	BD Biosciences	Cat.#555346 RRID:AB_395751	FC (1:30)
Antibody	mouse monoclonal anti-human CD4 (BV510)	BD Biosciences	Cat.#562970 RRID:AB_2744424	FC (1:300)
Antibody	mouse monoclonal anti-human CD45RA (PE-Texas-Red)	Invitrogen	Cat.#MHCD45RA17 RRID:AB_10372222	FC (1:200)
Antibody	mouse monoclonal anti-human CD8 (APC-H7)	BD Biosciences	Cat.#560179 RRID:AB_1645481	FC (1:100)
Antibody	mouse monoclonal anti-human CD8 (PE-Cy7)	BD Biosciences	Cat.#557746 RRID:AB_396852	FC (1:320)
Antibody	mouse monoclonal anti-human CD8 (Pacific Blue)	BD Biosciences	Cat.#558207 RRID:AB_397058	FC (1:500)
Antibody	mouse monoclonal anti-human IFN- γ (Alexa-Fluor 700)	Sony	Cat.#3112600 RRID:AB_2922770	FC (1:120)
Antibody	mouse monoclonal anti-human IFN- γ (BV711)	BD Biosciences	Cat.#564039 RRID:AB_2738557	FC (1:300)

Key Resourced Table *Continued*

Key Resources Table				
Reagent type (species) or resource	Designation	Source or reference	Identifiers	Additional information
Antibody	mouse monoclonal anti-human HLA-DR (Alexa-Fluor 700)	BD Biosciences	Cat.#560743 RRID:AB_1727526	FC (1:150)
Antibody	mouse monoclonal anti-human CD38 (BV605)	BD Biosciences	Cat.#740401 RRID:AB_2740131	FC (1:120)
Antibody	rat monoclonal anti- mouse CD19 (Mouse)	Biolegend	Cat.#557399 RRID:AB_396682	FC (1:250)
Other	Zombie-Red	Biolegend	Cat.#423109	FC (1:1000)
Other	Zombie-Aqua	BD Biosciences	Cat.#423101	FC (1:1000)
Other	Brilliant Violet Staining Buffer Plus	Beckham Coulter	Cat.#566385	FC (1:10)
Cell line (<i>Homo Sapiens</i>)	K-562	ATCC	CCL-342	
Cell line (<i>Homo Sapiens</i>)	Calu-3	ATCC	HTB-55	
Biological sample (<i>Homo Sapiens</i>)	PBMCs from 67 healthy donors	LUMC Biobank		Cryo- preserved before May 2019
Biological sample (<i>Homo Sapiens</i>)	PBMCs from critical COVID-19 patient (KDH)	LUMC BEAT-COVID consortium	Clinical trial #: NL8589	Male, 61 years, 31 days ICU
Biological sample (<i>Homo Sapiens</i>)	PBMCs from critical COVID-19 patient (CHZ)	LUMC BEAT-COVID consortium	Clinical trial #: NL8589	Male, 76 years, 40 days ICU
Biological sample (<i>Homo Sapiens</i>)	PBMCs from critical COVID-19 patient (CLS)	LUMC BEAT-COVID consortium	Clinical trial #: NL8589	Male, 71 years, 107 days ICU

Study samples and cell lines

Bio-banked PBMCs were cryopreserved after informed consent from the respective donors, in accordance with the declaration of Helsinki. The samples from COVID-19 patients were part of a trial (NL8589) registered in the Dutch Trial Registry and approved by Medical Ethical Committee Leiden-Den Haag-Delft (NL73740.058.20). All three patients suffered from critical COVID-19 as categorized according to World Health Organization guidelines (WHO ref#: WHO/2019-nCoV/clinical/2020.4) (see **Supplementary file 1** for patient details). Bio-banked PBMCs from CMV-seropositive (N=28) and CMV-seronegative (N=39) donors that were frozen down before May 2019 were randomly selected to assure that the samples are SARS-CoV-2 naïve and represent the European population (**Supplementary file 2**). Prior to cryopreservation, PBMCs were isolated from fresh whole blood using Ficoll-Isopaque. PBMCs were thawed in culture medium consisting of Iscove Modified Dulbecco Medium (IMDM; Lonza, Basel, Switzerland) supplemented with 10% heat-inactivated fetal bovine serum (FBS; Sigma-Aldrich, Saint Louis, Missouri), 2.7 mM L-glutamine (Lonza), 100 U/mL penicillin (Lonza) and 100 µg/mL streptomycin (Lonza) (1% p/s), and subsequently treated with 1.33 mg/ml DNase to minimize cell clumping. K562 cells (*CCL-243*; American Type Culture Collection (ATCC)) and Calu-3 lung carcinoma cells (*HTB-55*; ATCC) were regularly checked for the presence of mycoplasma. K562s were regularly checked to ensure (lack of) HLA expression and calu-3 cells were authenticated by STR sequencing.

Intracellular cytokine staining assay

Thawed PBMCs were stimulated in culture medium supplemented with 1 µg/mL SARS-CoV-2 peptides pools covering the entire spike (Miltenyi, Keulen, Germany), membrane (Miltenyi), or nucleocapsid (Miltenyi) proteins for one hour at 37°C + 5% CO₂. The peptides of the spike gene were by the manufacturer divided over a "S", "S1" and "S+" pool, wherein "S" covers the most immunogenic parts of the gene, "S1" mostly covers S1 domain and "S+" mostly covers S2 domain. An additional peptide pool containing 11 amino acid overlapping 15-mer peptides covering the pp65 antigen from CMV (JPT Peptide Technologies) was included (see **Supplementary file 3** for peptide details). After one hour stimulation, 5 µg/mL Brefeldin A (Sigma-Aldrich) was added and the samples were incubated for an additional 15 hours at 37°C + 5% CO₂. The samples were subsequently stained with the viability dye Zombie-Red (Biolegend, San Diego, California) for 25 minutes at room temperature (RT) after which the cells were washed in PBS containing 0.8 mg/mL albumin (FACS buffer) and stained with antibodies against CD4 and CD8 in FACS buffer for 30 minutes at 4°C. Cells were washed in PBS and fixed in 1% paraformaldehyde for 8 minutes RT followed by a wash and a permeabilization step for 30 minutes at 4°C in FACS

buffer supplemented with 1% p/s and 0.1% saponin (permeabilization buffer). After permeabilization, the cells were stained using an antibody cocktail directed against CD14, CD19, CD137, CD154 and IFN- γ in permeabilization buffer (see **Supplementary file 4** for antibody details) for 30 minutes at 4°C. After staining, the samples were washed, resuspended in permeabilization buffer and measured on a 3-laser aurora (Cytek Biosciences, Fremont, California).

Isolation of SARS-CoV-2-specific T cells

Thawed PBMCs were stimulated for 16 hours at 37°C + 5% CO₂ using 1 μ g/mL of spike (Miltenyi) or membrane (Miltenyi) peptide pool in culture medium (see **Supplementary file 7** for peptide details). After stimulation, the cells were washed and stained with antibodies directed against CD4, CD8 and CD137 in phenol-red free IMDM (Gibco, Waltham, Massachusetts) containing 2% FBS (Sigma-Aldrich), 1% p/s (Lonza) (sort medium) (see **Supplementary file 4** for antibody details) for 30 minutes at 4°C. The cells were subsequently washed and resuspended in sort medium. CD4 $^{+}$ or CD8 $^{+}$ and CD137 $^{+}$ cells were single-cell sorted using an Aria III cell sorter (BD Biosciences, Franklin Lakes, New Jersey) into a 96-well round-bottom plate containing 1x10⁵ 35-Gy-irradiated PBMCs, 50-Gy-irradiated EBV-LCL-JYs and 0.8 μ g/mL phytohemagglutinin (PHA) (Thermo Fisher, Waltham, Massachusetts) in 100 μ L T cell medium (TCM) consisting of IMDM (Lonza) supplemented with 2.7 mM L-glutamine (Lonza), 100 U/mL penicillin (Lonza) and 100 μ g/mL streptomycin (Lonza), 5% FBS (Sigma-Aldrich), 5% human serum (Sanquin, Amsterdam, The Netherlands) and 100 IU/mL recombinant human IL-2 (Novartis, Basel, Switzerland). Sorted T cells were clonally expanded to generate T cell clones. T cell clones were restimulated between day 14-20 post stimulation using PHA, PBMCs and EBV-LCL-JYs as described above and used for assays between day 7-20 post stimulation.

Co-culture assays

To test peptide and HLA restriction, T cell clones were washed and co-cultured with stimulator cells in a 1:6 effector to stimulator ratio. Stimulator cells consisted of either autologous or HLA-matched EBV-LCLs or retrovirally transduced K562s. K562 were transduced with a pZLRS or MP71 vector containing a HLA gene of interested linked to a marker gene, transduction was performed as previously described ⁶⁴. Cells were enriched for marker gene expression using magnetic activated cell sorting (MACS; Miltenyi) or fluorescent activated cell sorting (FACS) on an Aria III cell sorter (BD Biosciences). Stimulator cells were loaded with peptides through pre-incubation for 30 minutes at 37°C with 0.01-1 μ M peptide (**Supplementary file 3** for peptide details). To identify the pp65 epitope of the CD4 $^{+}$ T cell clones, a co-culture assay was performed using a pp65 peptide library. The pp65 library consisted of 15-mer

peptides with 11 amino acid overlap, spanning the whole pp65 gene. The peptides are divided into matrix pools with horizontal and vertical sub pools so that each pool has an unique peptide combination and each peptide is in one horizontal and one vertical sub pool. To identify the HLA-restriction of the CD4⁺ T cell clones, the peptides were not washed away during the co-culture incubation period and HLA class II was knocked out in the T cell clones as previously described ⁶⁵. However, the protocol was adapted to knock-out Class II Major histocompatibility complex transactivator (CIITA) by designing two reverse guide RNAs: 5'-AGTCGCTCACTGGTCCCCTAGG-3' and 5'-CCGTGGACAGTGAATCCACTGGG-3' (Integrated DNA technologies Inc., Coralville, Iowa). Co-culture assays were incubated overnight and secreted IFN- γ was measured as an indicator of T cell activity by ELISA (Diaclone, Besançon, France) as described by the manufacturer.

To identify the peptide recognition signature of the CD8 T cell clones, a co-culture assay was performed using a nonamer combinatorial peptide library (CPL) ³⁵. The 9-mer CPL scan contains 180 peptide pools with each pool consisting of a mixture of peptides with one naturally-occurring amino acid fixed at one position ⁶⁶. Co-culture assay was performed as described above with small changes; 2x10⁴ K562 transduced with HLA-B*35:01 were pre-incubated with 100 μ M CPL peptides for 1 hour at 37°C before 5x10³ T cell clones were added. After overnight incubation, secreted IFN- γ was measured by an IFN- γ -ELISA (Diaclone) and results were analyzed using WSBC PI CPL for viruses ^{67,68}. Identified peptides following peptide libraries or CPL were analyzed for predicted binding to HLA-B*35:01 using netMHC 4.0 ⁶⁹. Alternatively, peptide recognition by T cell clones was measured using ICS assay as described above.

Peptide-HLA modelling

The binding of FVS in HLA-B*35:01 was modelled based on the solved crystal structure of the HLA-B*35:01-IPS ⁴⁵. Each residue of the IPS peptide was mutated to their corresponding residues in the FVS peptide using the mutagenesis wizard in PyMOL ⁷⁰. The residues were mutated into the most favorable rotamer to avoid steric clashes. No major steric clashes with the peptide or HLA were observed.

Tetramer staining

1-2x10⁶ PBMCs or 5x10⁴ T cell clones were incubated with in-house generated, PE- or APC-conjugated tetramers for 30 minutes at RT ⁵³. After tetramer incubation, the cells were washed and incubated with an antibody mix targeting CD4, CD8, CD45RA, CCR7, CD38 and/or HLA-DR. After incubation, cells were washed and resuspended in FACS buffer and immediately measured on a 3-laser Aurora (Cytek Biosciences).

TCR sequencing

PBMCs were thawed and 10-50x10⁶ cells directly stained with PE-conjugated HLA-B*35:01-FVS or HLA-B*35:01-IPS tetramers. Tetramers were labelled to beads using anti-PE MicroBeads (Miltenyi) and enriched through magnetic-activated cell sorting (Miltenyi). The tetramer-enriched cells were washed and incubated with an antibody cocktail targeting CD4 and CD8 (see **Supplementary file 4** for antibody details) in sort medium. Stained samples were washed in sort medium and bulk-sorted on an Aria III cell sorter (BD Biosciences) (see **Fig S6B** for a gating example). RNA isolation and TCR sequencing was performed as previously described ⁷¹. In short, cells were directly collected in lysis buffer for RNA isolation using the ReliaPrep RNA cell Miniprep system (Promega, Madison, Wisconsin). The total RNA yield of each sample was converted to cDNA using a template-switch oligo primer (TSO) (Eurogentec, Seraing, Belgium), RNasin (Promega) and SMARTScribe reverse transcriptase (Takara Bio, Kusatsu, Japan) ⁷². cDNA was pre-amplified via an IS region in the Oligo dT primer prior to barcoding on samples containing cDNA from 500 or fewer cells ⁷³. Barcoded TCR PCR product was generated in two rounds of PCR: in the first PCR reaction, *TRA* and *TRB* product was generated in separate PCR reactions using Phusion Flash (Thermo Fisher Scientific), Smartseq2modified PCR primer (Eurogentec) and TRAC or TRBC1/2 specific primers (Eurogentec) (see **Supplementary file 5** for primer list). The PCR product was then purified using the Wizard SV 96 PCR Clean-Up System (Promega) and barcoded in a second PCR using two-sided six-nucleotide barcoded primers to discriminate between TCRs of different T cell populations. PCR products of different T cell populations were pooled, after which TCR sequences were identified by NovaSeq (GenomeScan, Leiden, The Netherlands).

SARS-CoV-2 infection assay

Calu-3 lung carcinoma cells (HTB-55; ATCC) were cultured in Eagle's minimum essential medium (EMEM, Lonza), supplemented with 9% fetal calf serum (FCS; CapriCorn Scientific, USA), 1% NEAA (Sigma-Aldrich), 2 mM L-glutamine (Sigma-Aldrich), 1 mM sodium pyruvate (Sigma-Aldrich) and 100 U/ml of penicillin/streptomycin (P/S; Sigma-Aldrich). Calu-3 cells were retrovirally transduced with a pLZRS vector containing the HLA-B*35:01 molecule linked via an internal ribosome entry site (IRES) sequence to mouse CD19, transduction was performed as previously described ⁶⁴. Mouse CD19 was used as a marker gene to enrich for successfully transduced cells by adding antibodies directed against mouse CD19 and enriching for stained cells by MACS (Miltenyi) followed by FACS on an Aria III cell sorter (BD Biosciences) (see **Supplementary file 4** for antibody details). For the infection assay, Calu-3 cells were seeded in 96-well cell culture plates at a density of 3x10⁴ cells per well in 100 µl culture medium. Infections were done with clinical isolate SARS-CoV-2/Leiden-0008,

which was isolated from a nasopharyngeal sample collected at the LUMC during the first wave of the Corona pandemic in March 2020 (GenBack: MT705206.1). Cells were infected with SARS-CoV-2 at a multiplicity of infection (MOI) of 0.05 or 0.5 in 50 μ l infection medium. After 1.5h, cells were washed three times with medium and 100 μ l of medium was added. At 6 hours post infection (hpi) medium was removed again and 100 μ l of T cell medium with 3×10^5 T cells per well was added. At 24 hpi cells were harvested to collect intracellular RNA by lysing the cells in 100 μ l GITC reagent (3M GITC, 2% sarkosyl, 20 mM Tris, 20 mM EDTA) per well. Intracellular RNA was isolated using magnetic beads and viral RNA was quantified by internally controlled multiplex TaqMan RT-qPCR as described previously ⁷⁴.

2

Statistics

Flow cytometry data was unmixed using Spectroflo (Cytek Biosciences) and analyzed using FlowJo v10.7.1. (BD Biosciences) to set gates on the samples based on the DMSO negative control in ICS assays or adapted to positive control for tetramer staining (see **Figure 1 – figure supplement 1**, **figure 2 – figure supplement 1**, **figure 4 – figure supplement 1** and **figure 5 – figure supplement 1** for a gating example). Samples were excluded from the analysis if less than 10,000 events in CD4 $^+$ or CD8 $^+$ gate was measured or if after further testing they appeared not to be $\alpha\beta$ T cells. For the SARS-CoV-2 infection assays, experiments were excluded from the analysis if the positive control had higher SARS-CoV-2 intracellular RNA copies compared to no T cell condition. Statistical analysis and generation of figures was conducted using GraphPad Prism 9.0.1 (GraphPad Software). Data was tested for significance using an one-way ANOVA with *p*-values below 0.05 considered as significant. *p*-values are categorized in the figures as: ns=not significant; **p*<0.05; ***p*<0.01 or ****p*<0.001.

TCR sequence data were analysed using MiXCR software (v3.0.13) to determine the V α and V β family and CDR3 regions using annotation of the IMGT library (<http://www.imgt.org; v6>)⁷⁵. CDR3 regions were analysed in RStudio and CDR3 sequences that were non-functional or had ≤ 50 reads were excluded from the analysis.

Acknowledgements

The authors like to thank Joost M. Lambooij for critically editing the manuscript. Flow cytometry was performed at the Flow cytometry Core Facility (FCF) of Leiden University Medical Center (LUMC) in Leiden, Netherlands (<https://www.lumc.nl/research/facilities/fcf>).

REFERENCES

1. Brodin, P. Immune determinants of COVID-19 disease presentation and severity. *Nat Med* **27**, 28-33, doi:10.1038/s41591-020-01202-8 (2021).
2. Sette, A. & Crotty, S. Adaptive immunity to SARS-CoV-2 and COVID-19. *Cell* **184**, 861-880, doi:10.1016/j.cell.2021.01.007 (2021).
3. Liao, M. *et al.* Single-cell landscape of bronchoalveolar immune cells in patients with COVID-19. *Nat Med* **26**, 842-844, doi:10.1038/s41591-020-0901-9 (2020).
4. Rydzynski Moderbacher, C. *et al.* Antigen-Specific Adaptive Immunity to SARS-CoV-2 in Acute COVID-19 and Associations with Age and Disease Severity. *Cell* **183**, 996-1012 e1019, doi:10.1016/j.cell.2020.09.038 (2020).
5. Sekine, T. *et al.* Robust T Cell Immunity in Convalescent Individuals with Asymptomatic or Mild COVID-19. *Cell* **183**, 158-168 e114, doi:10.1016/j.cell.2020.08.017 (2020).
6. Bange, E. M. *et al.* CD8(+) T cells contribute to survival in patients with COVID-19 and hematologic cancer. *Nat Med* **27**, 1280-1289, doi:10.1038/s41591-021-01386-7 (2021).
7. Tan, A. T. *et al.* Early induction of functional SARS-CoV-2-specific T cells associates with rapid viral clearance and mild disease in COVID-19 patients. *Cell Rep* **34**, 108728, doi:10.1016/j.celrep.2021.108728 (2021).
8. Bertoletti, A., Le Bert, N., Qui, M. & Tan, A. T. SARS-CoV-2-specific T cells in infection and vaccination. *Cell Mol Immunol* **18**, 2307-2312, doi:10.1038/s41423-021-00743-3 (2021).
9. Gao, Y. *et al.* Ancestral SARS-CoV-2-specific T cells cross-recognize the Omicron variant. *Nat Med*, doi:10.1038/s41591-022-01700-x (2022).
10. Keeton, R. *et al.* T cell responses to SARS-CoV-2 spike cross-recognize Omicron. *Nature*, doi:10.1038/s41586-022-04460-3 (2022).
11. Liu, J. *et al.* Vaccines Elicit Highly Conserved Cellular Immunity to SARS-CoV-2 Omicron. *Nature*, doi:10.1038/s41586-022-04465-y (2022).
12. GeurtsvanKessel, C. H. *et al.* Divergent SARS CoV-2 Omicron-reactive T- and B cell responses in COVID-19 vaccine recipients. *Sci Immunol*, eabo2202, doi:10.1126/sciimmunol.abo2202 (2022).
13. Tarke, A. *et al.* SARS-CoV-2 vaccination induces immunological T cell memory able to cross-recognize variants from Alpha to Omicron. *Cell*, doi:10.1016/j.cell.2022.01.015 (2022).
14. Chiuppesi, F. *et al.* Vaccine-induced spike- and nucleocapsid-specific cellular responses maintain potent cross-reactivity to SARS-CoV-2 Delta and Omicron variants. *iScience* **25**, 104745, doi:10.1016/j.isci.2022.104745 (2022).
15. Choi, S. J. *et al.* T cell epitopes in SARS-CoV-2 proteins are substantially conserved in the Omicron variant. *Cell Mol Immunol* **19**, 447-448, doi:10.1038/s41423-022-00838-5 (2022).
16. Jung, M. K. *et al.* BNT162b2-induced memory T cells respond to the Omicron variant with preserved polyfunctionality. *Nature Microbiology* **7**, 909-917 (2022).
17. Redd, A. D. *et al.* Minimal Crossover between Mutations Associated with Omicron Variant of SARS-CoV-2 and CD8(+) T-Cell Epitopes Identified in COVID-19 Convalescent Individuals. *mbio* **13**, e0361721, doi:10.1128/mbio.03617-21 (2022).

18. Grifoni, A. *et al.* Targets of T Cell Responses to SARS-CoV-2 Coronavirus in Humans with COVID-19 Disease and Unexposed Individuals. *Cell* **181**, 1489-1501 e1415, doi:10.1016/j.cell.2020.05.015 (2020).

19. Weiskopf, D. *et al.* Phenotype and kinetics of SARS-CoV-2-specific T cells in COVID-19 patients with acute respiratory distress syndrome. *Sci Immunol* **5**, doi:10.1126/sciimmunol.abd2071 (2020).

20. Nelde, A. *et al.* SARS-CoV-2-derived peptides define heterologous and COVID-19-induced T cell recognition. *Nat Immunol* **22**, 74-85, doi:10.1038/s41590-020-00808-x (2021).

21. Mateus, J. *et al.* Selective and cross-reactive SARS-CoV-2 T cell epitopes in unexposed humans. *Science* **370**, 89-94, doi:10.1126/science.abd3871 (2020).

22. Le Bert, N. *et al.* SARS-CoV-2-specific T cell immunity in cases of COVID-19 and SARS, and uninfected controls. *Nature* **584**, 457-462, doi:10.1038/s41586-020-2550-z (2020).

23. Braun, J. *et al.* SARS-CoV-2-reactive T cells in healthy donors and patients with COVID-19. *Nature* **587**, 270-274, doi:10.1038/s41586-020-2598-9 (2020).

24. Kundu, R. *et al.* Cross-reactive memory T cells associate with protection against SARS-CoV-2 infection in COVID-19 contacts. *Nat Commun* **13**, 80, doi:10.1038/s41467-021-27674-x (2022).

25. Loyal, L. *et al.* Cross-reactive CD4(+) T cells enhance SARS-CoV-2 immune responses upon infection and vaccination. *Science* **374**, eabh1823, doi:10.1126/science.abh1823 (2021).

26. Bacher, P. *et al.* Low-Avidity CD4(+) T Cell Responses to SARS-CoV-2 in Unexposed Individuals and Humans with Severe COVID-19. *Immunity* **53**, 1258-1271 e1255, doi:10.1016/j.jimmuni.2020.11.016 (2020).

27. Johansson, A. M. *et al.* Cross-reactive and mono-reactive SARS-CoV-2 CD4+ T cells in prepandemic and COVID-19 convalescent individuals. *PLoS Pathog* **17**, e1010203, doi:10.1371/journal.ppat.1010203 (2021).

28. Tan, C. C. S. *et al.* Pre-existing T cell-mediated cross-reactivity to SARS-CoV-2 cannot solely be explained by prior exposure to endemic human coronaviruses. *Infect Genet Evol* **95**, 105075, doi:10.1016/j.meegid.2021.105075 (2021).

29. Peng, Y. *et al.* Broad and strong memory CD4(+) and CD8(+) T cells induced by SARS-CoV-2 in UK convalescent individuals following COVID-19. *Nat Immunol* **21**, 1336-1345, doi:10.1038/s41590-020-0782-6 (2020).

30. Stervbo, U., Rahmann, S., Roch, T., Westhoff, T. H. & Babel, N. Epitope similarity cannot explain the pre-formed T cell immunity towards structural SARS-CoV-2 proteins. *Sci Rep* **10**, 18995, doi:10.1038/s41598-020-75972-z (2020).

31. Clute, S. C. *et al.* Cross-reactive influenza virus-specific CD8+ T cells contribute to lymphoproliferation in Epstein-Barr virus-associated infectious mononucleosis. *J Clin Invest* **115**, 3602-3612, doi:10.1172/JCI25078 (2005).

32. Riley, T. P. *et al.* T cell receptor cross-reactivity expanded by dramatic peptide-MHC adaptability. *Nat Chem Biol* **14**, 934-942, doi:10.1038/s41589-018-0130-4 (2018).

33. Su, L. F. & Davis, M. M. Antiviral memory phenotype T cells in unexposed adults. *Immunol Rev* **255**, 95-109, doi:10.1111/imr.12095 (2013).

34. Cameron, B. J. *et al.* Identification of a Titin-derived HLA-A1-presented peptide as a cross-reactive target for engineered MAGE A3-directed T cells. *Sci Transl Med* **5**, 197ra103, doi:10.1126/scitranslmed.3006034 (2013).

35. Bijen, H. M. *et al.* Preclinical Strategies to Identify Off-Target Toxicity of High-Affinity TCRs. *Mol Ther* **26**, 1206-1214, doi:10.1016/j.mtthe.2018.02.017 (2018).

36. Cornberg, M. *et al.* CD8 T cell cross-reactivity networks mediate heterologous immunity in human EBV and murine vaccinia virus infections. *J Immunol* **184**, 2825-2838, doi:10.4049/jimmunol.0902168 (2010).

37. Lee, C. H. *et al.* Predicting Cross-Reactivity and Antigen Specificity of T Cell Receptors. *Front Immunol* **11**, 565096, doi:10.3389/fimmu.2020.565096 (2020).

38. Meckiff, B. J. *et al.* Imbalance of Regulatory and Cytotoxic SARS-CoV-2-Reactive CD4(+) T Cells in COVID-19. *Cell* **183**, 1340-1353 e1316, doi:10.1016/j.cell.2020.10.001 (2020).

39. Zuhair, M. *et al.* Estimation of the worldwide seroprevalence of cytomegalovirus: A systematic review and meta-analysis. *Rev Med Virol* **29**, e2034, doi:10.1002/rmv.2034 (2019).

40. Sylwester, A. W. *et al.* Broadly targeted human cytomegalovirus-specific CD4+ and CD8+ T cells dominate the memory compartments of exposed subjects. *J Exp Med* **202**, 673-685, doi:10.1084/jem.20050882 (2005).

41. Alanio, C. *et al.* Cytomegalovirus latent infection is associated with an increased risk of COVID-19-related hospitalization. *J Infect Dis*, doi:10.1093/infdis/jiac020 (2022).

42. Weber, S. *et al.* CMV seropositivity is a potential novel risk factor for severe COVID-19 in non-geriatric patients. *PLoS One* **17**, e0268530, doi:10.1371/journal.pone.0268530 (2022).

43. Jo, N. *et al.* Aging and CMV Infection Affect Pre-existing SARS-CoV-2-Reactive CD8+ T Cells in Unexposed Individuals. *Frontiers in Aging* **2**, doi:10.3389/fragi.2021.719342 (2021).

44. Klarenbeek, P. L. *et al.* Deep sequencing of antiviral T-cell responses to HCMV and EBV in humans reveals a stable repertoire that is maintained for many years. *PLoS Pathog* **8**, e1002889, doi:10.1371/journal.ppat.1002889 (2012).

45. Pellicci, D. G. *et al.* The molecular bases of delta/alphabeta T cell-mediated antigen recognition. *J Exp Med* **211**, 2599-2615, doi:10.1084/jem.20141764 (2014).

46. Nguyen, A. T. *et al.* SARS-CoV-2 Spike-Derived Peptides Presented by HLA Molecules. *Biophysica* **1**, 194-203 (2021).

47. Escobar, H. *et al.* Large scale mass spectrometric profiling of peptides eluted from HLA molecules reveals N-terminal-extended peptide motifs. *J Immunol* **181**, 4874-4882, doi:10.4049/jimmunol.181.7.4874 (2008).

48. Tarke, A. *et al.* Comprehensive analysis of T cell immunodominance and immunoprevalence of SARS-CoV-2 epitopes in COVID-19 cases. *Cell Rep Med* **2**, 100204, doi:10.1016/j.xcrm.2021.100204 (2021).

49. Shomuradova, A. S. *et al.* SARS-CoV-2 Epitopes Are Recognized by a Public and Diverse Repertoire of Human T Cell Receptors. *Immunity* **53**, 1245-1257 e1245, doi:10.1016/j.immuni.2020.11.004 (2020).

50. Lineburg, K. E. *et al.* CD8(+) T cells specific for an immunodominant SARS-CoV-2 nucleocapsid epitope cross-react with selective seasonal coronaviruses. *Immunity* **54**, 1055-1065 e1055, doi:10.1016/j.immuni.2021.04.006 (2021).

51. Price, D. A. *et al.* Avidity for antigen shapes clonal dominance in CD8+ T cell populations specific for persistent DNA viruses. *J Exp Med* **202**, 1349-1361, doi:10.1084/jem.20051357 (2005).

52. Abdel-Hakeem, M. S., Boisvert, M., Bruneau, J., Soudeyns, H. & Shoukry, N. H. Selective expansion of high functional avidity memory CD8 T cell clonotypes during hepatitis C virus reinfection and clearance. *PLoS Pathog* **13**, e1006191, doi:10.1371/journal.ppat.1006191 (2017).

53. Hombrink, P. *et al.* Mixed functional characteristics correlating with TCR-ligand koff -rate of MHC-tetramer reactive T cells within the naive T-cell repertoire. *Eur J Immunol* **43**, 3038-3050, doi:10.1002/eji.201343397 (2013).

54. Schober, K., Buchholz, V. R. & Busch, D. H. TCR repertoire evolution during maintenance of CMV-specific T-cell populations. *Immunol Rev* **283**, 113-128, doi:10.1111/imr.12654 (2018).

55. Gao, Z. *et al.* A systematic review of asymptomatic infections with COVID-19. *J Microbiol Immunol Infect* **54**, 12-16, doi:10.1016/j.jmii.2020.05.001 (2021).

56. Steiner, S. *et al.* Reactive T Cells in Convalescent COVID-19 Patients With Negative SARS-CoV-2 Antibody Serology. *Front Immunol* **12**, 687449, doi:10.3389/fimmu.2021.687449 (2021).

57. Cusick, M. F., Libbey, J. E. & Fujinami, R. S. Molecular mimicry as a mechanism of autoimmune disease. *Clin Rev Allergy Immunol* **42**, 102-111, doi:10.1007/s12016-011-8293-810.1007/s12016-011-8294-7 (2012).

58. Macdonald, W. A. *et al.* T cell allorecognition via molecular mimicry. *Immunity* **31**, 897-908, doi:10.1016/j.jimmuni.2009.09.025 (2009).

59. Cole, D. K. *et al.* Hotspot autoimmune T cell receptor binding underlies pathogen and insulin peptide cross-reactivity. *J Clin Invest* **126**, 3626, doi:10.1172/JCI89919 (2016).

60. Birnbaum, M. E. *et al.* Deconstructing the peptide-MHC specificity of T cell recognition. *Cell* **157**, 1073-1087, doi:10.1016/j.cell.2014.03.047 (2014).

61. Adams, J. J. *et al.* T cell receptor signaling is limited by docking geometry to peptide-major histocompatibility complex. *Immunity* **35**, 681-693, doi:10.1016/j.jimmuni.2011.09.013 (2011).

62. Piepenbrink, K. H., Blevins, S. J., Scott, D. R. & Baker, B. M. The basis for limited specificity and MHC restriction in a T cell receptor interface. *Nat Commun* **4**, 1948, doi:10.1038/ncomms2948 (2013).

63. Szeto, C., Lobos, C. A., Nguyen, A. T. & Gras, S. TCR Recognition of Peptide-MHC-I: Rule Makers and Breakers. *Int J Mol Sci* **22**, doi:10.3390/ijms22010068 (2020).

64. Jahn, L. *et al.* Therapeutic targeting of the BCR-associated protein CD79b in a TCR-based approach is hampered by aberrant expression of CD79b. *Blood* **125**, 949-958, doi:10.1182/blood-2014-07-587840 (2015).

65. Morton, L. T. *et al.* Simultaneous Deletion of Endogenous TCRalphabeta for TCR Gene Therapy Creates an Improved and Safe Cellular Therapeutic. *Mol Ther* **28**, 64-74, doi:10.1016/j.ymthe.2019.10.001 (2020).

66. Wooldridge, L. *et al.* CD8 controls T cell cross-reactivity. *J Immunol* **185**, 4625-4632, doi:10.4049/jimmunol.1001480 (2010).

67. Szomolay, B. *et al.* Identification of human viral protein-derived ligands recognized by individual MHC-I-restricted T-cell receptors. *Immunol Cell Biol* **94**, 573-582, doi:10.1038/icb.2016.12 (2016).

68. Wooldridge, L. Individual MHC-I-Restricted T-Cell Receptors are Characterized by a Unique Peptide Recognition Signature. *Front Immunol* **4**, 199, doi:10.3389/fimmu.2013.00199 (2013).

69. Andreatta, M. & Nielsen, M. Gapped sequence alignment using artificial neural networks: application to the MHC class I system. *Bioinformatics* **32**, 511-517, doi:10.1093/bioinformatics/btv639 (2016).

70. Schrodinger, LLC. *The PyMOL Molecular Graphics System, Version 1.8* (2015).
71. Roukens, A. H. E. *et al.* Prolonged activation of nasal immune cell populations and development of tissue-resident SARS-CoV-2-specific CD8(+) T cell responses following COVID-19. *Nat Immunol* **23**, 23-32, doi:10.1038/s41590-021-01095-w (2022).
72. Koning, M. T. *et al.* ARTISAN PCR: rapid identification of full-length immunoglobulin rearrangements without primer binding bias. *Br J Haematol* **178**, 983-986, doi:10.1111/bjh.14180 (2017).
73. Picelli, S. *et al.* Smart-seq2 for sensitive full-length transcriptome profiling in single cells. *Nat Methods* **10**, 1096-1098, doi:10.1038/nmeth.2639 (2013).
74. Salgado-Benvindo, C. *et al.* Suramin Inhibits SARS-CoV-2 Infection in Cell Culture by Interfering with Early Steps of the Replication Cycle. *Antimicrob Agents Ch* **64**, doi:ARTN e00900-2010.1128/AAC.00900-20 (2020).
75. Bolotin, D. A. *et al.* MiXCR: software for comprehensive adaptive immunity profiling. *Nat Methods* **12**, 380-381, doi:10.1038/nmeth.3364 (2015).

SUPPLEMENTARY FIGURES

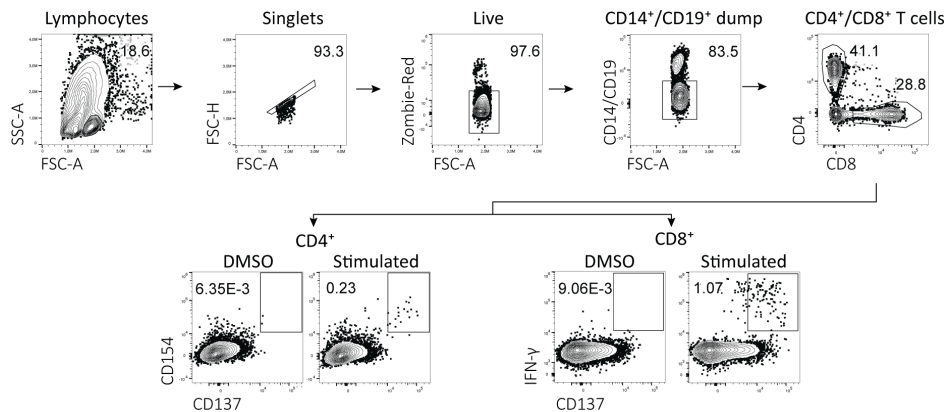


Figure 1 - figure supplement 1 Flow cytometry gating example for peptide stimulation assays

Representative example of flow cytometry gating strategy for peptide-reactive CD4⁺ and CD8⁺ T cells. All events were gated on lymphocytes, single cells, viable cells, CD14 and CD19 negative and either CD4 or CD8 positive. For CD4⁺ T cells, activation was measured by upregulation of CD137 and CD154 compared to DMSO. For CD8⁺ T cells, activation was measured by upregulation of CD137 and IFN- γ production compared to DMSO.

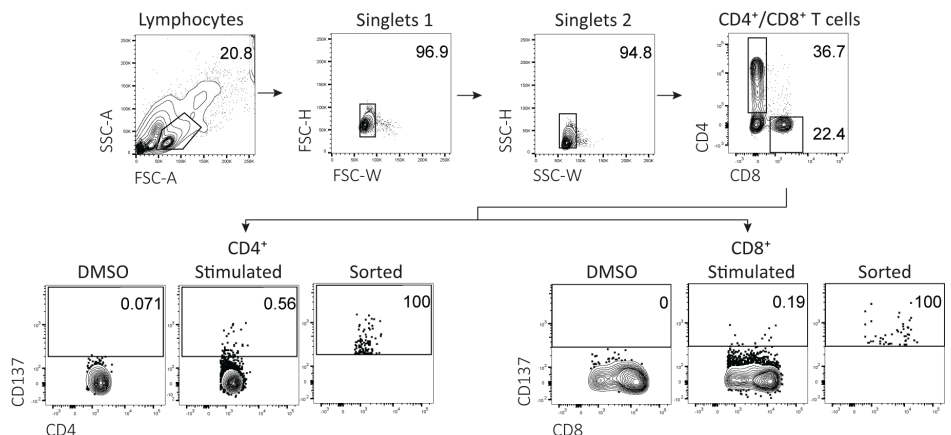


Figure 2 - figure supplement 1 Flow-activated cell sorting example for peptide stimulation assays

Representative example of fluorescent-activated cell sorting for peptide-reactive CD4⁺ and CD8⁺ T cells. All events were gated on lymphocytes, single cells and subsequently selected for CD4 positive or CD8 positive cells. Activated CD4⁺ or CD8⁺ T cells were sorted based on increased expression of CD137 compared to DMSO.

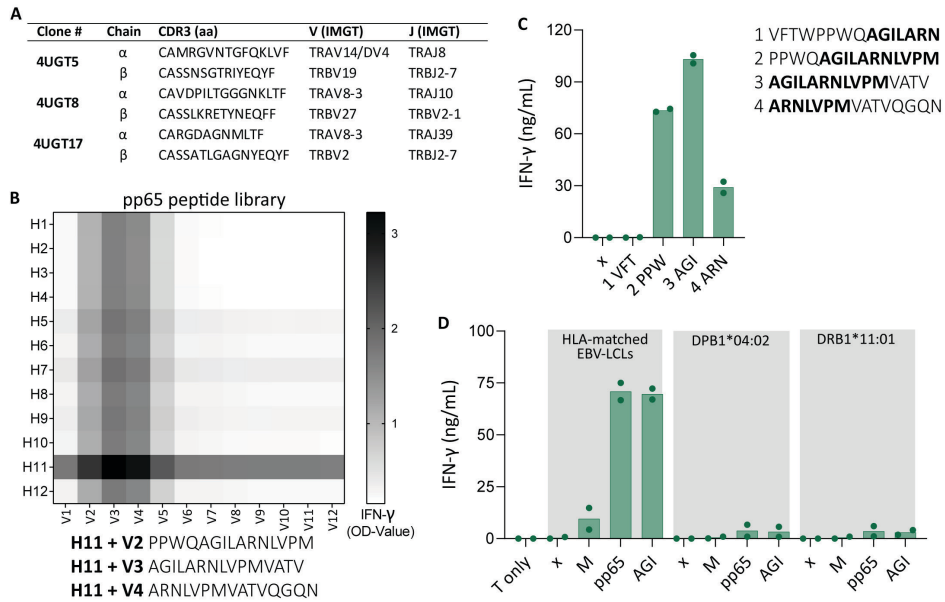


Figure 2 - figure supplement 2 TCR sequence and pp65 peptide identification of 4UGT8 clone

A) Figure showing T cell receptor sequencing of 3 cross-reactive CD4⁺ T cell clones. B) Heatmap showing reactivity of 4UGT8 clone after co-culturing with HLA-matched EBV-LCLs and CMV pp65 peptide library which consisted of 12 horizontal (H1-H12) and 12 vertical sub pools (V1-V12). Reactivity was measured by IFN- γ ELISA of the supernatant, depicted as OD-value. Peptides that were present in the sub pools with highest reactivity are shown below the figure. C) Bar graphs showing IFN- γ secretion after co-culturing 4UGT8 clone with single peptides. Peptide sequences are depicted next to the figure with amino acid overlap between the peptides in bold. Data points are technical duplicates. D) Bar graphs showing ELISA measurement of secreted IFN- γ after co-culturing of 4UGT8 clone with HLA-matched EBV-LCLs, or HLA-mismatched EBV-LCLs transduced with HLA-DPB1*04:02 or DRB1*11:01. Stimulator cells were peptide-pulsed with membrane (M) peptide pool, pp65 peptide pool or AGILARNLVPM (AGI) peptide. Data points are experimental duplicates. Black arrows indicate that values were above plateau value of the ELISA calibration curve.

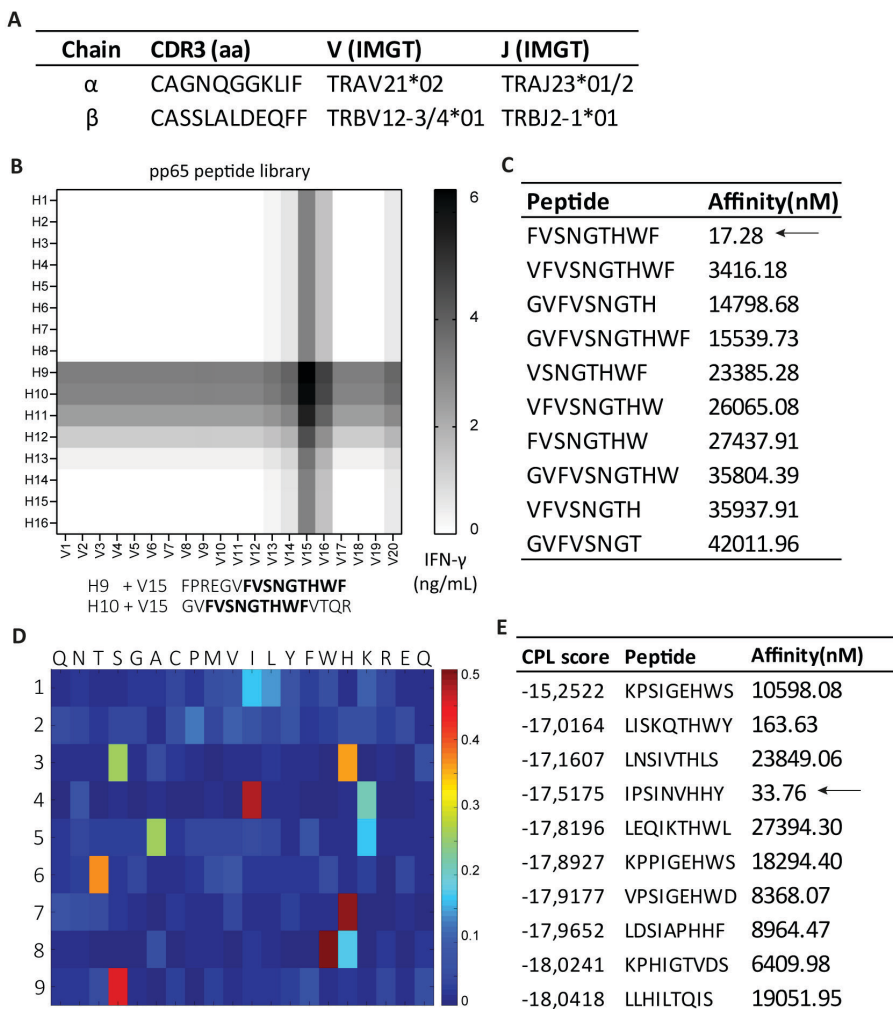


Figure 2 - figure supplement 3 TCR sequence and peptide identification of 8UTT6 clone

A) Figure showing T cell receptor sequencing result of UTT clones (N=23). B) Heatmap showing reactivity of a representative clone, 8UTT6 clone, against sub pools of SARS-CoV-2 spike peptide library loaded on K562s transduced with HLA-B*35:01. Reactivity was measured by IFN- γ ELISA. Peptides that induced highest IFN- γ production were depicted under the figure with amino acid overlap between the peptides in black. C) Figure showing NetMHC 4.0-predicted binding to HLA-B*35:01 of peptides that were recognized in the spike peptide library. The 10 peptides with highest binding to HLA-B*35:01 are shown and strong binders are indicated by an arrow. D) Heatmap demonstrating peptide recognition signature of 8UTT6 clone using the CPL assay. 8UTT6 clone was co-cultured with peptide-loaded K562 cells transduced HLA-B*35:01. Secreted IFN- γ was measured by ELISA and corrected per row. Y-axis shows peptide position and x-axis shows the fixed amino acid. E) Figure showing the 10 peptides with highest CPL score, their binding affinity to HLA-B*35:01 and strong binders are indicated by an arrow, as predicted by netMHC 4.0.

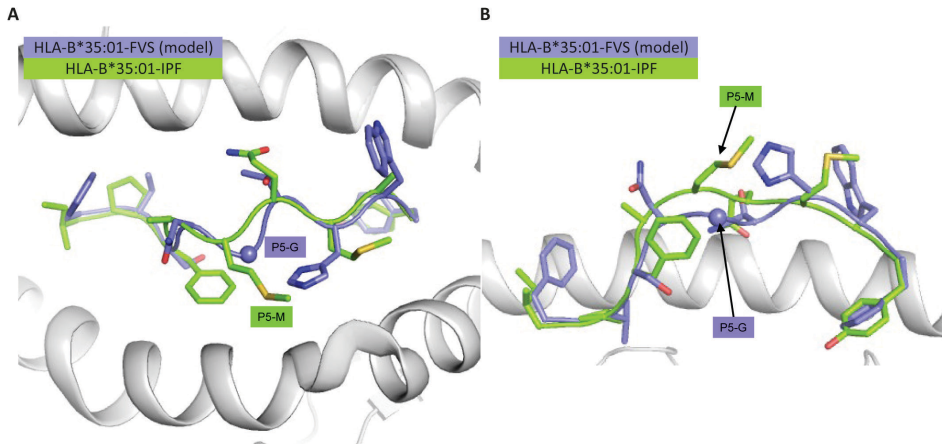


Figure 3 - figure supplement 1 Structural overlay of HLA-B*35:01-IPF structure with the model of the HLA-B*35:01-FVS

(A) Top view of the HLA-B*35:01-IPF (peptide in chartreuse) and HLA-B*35:01-FVS (peptide in blue) aligned on the HLA cleft (white cartoon). B) Side view of the same structural overlay as panel A, with the same colour scheme. The sphere represents the $C\alpha$ atom of the FVS peptide P5-G residue.

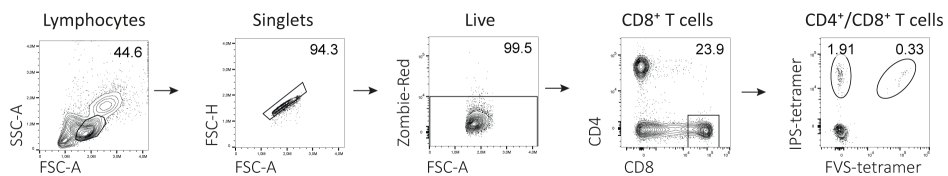


Figure 4 - figure supplement 1 Flow cytometry gating example for tetramer staining assays

Representative example of flow cytometry gating strategy for tetramer positive CD8⁺ T cells. All events were gated on lymphocytes, single cells, viable cells, CD8 positive and subsequently separated for binding to tetramer consisting of HLA-B*35:01 with IPS peptide or FVS peptide.

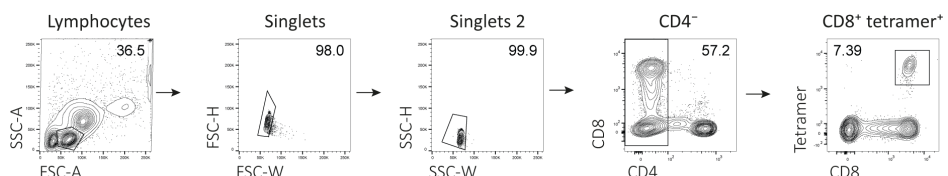


Figure 5 - figure supplement 1 Flow activated cell sorting gating example

Representative example of fluorescent-activated cell sorting for tetramer positive CD8⁺ T cells. All events were gated on lymphocytes, single cells, CD4⁻ and subsequently on CD8⁺tetramer⁺.

A

	TRAV (IMGT)	TRAJ (IMGT)	CDR3 (aa)	CDR3 α (nt)
UTT	TRAV21*02	TRAJ23*01	CGNQGGKLIF	T G T G C T G G G A A C C A G G G A G G A A A G C T T A T C T T C
UBV	TRAV21*01	TRAJ23*01	CGNQGGKLIF	T G T G C T G G A A A C C A G G G A G G A A A G C T T A T C T T C
JZX	TRAV21*02	TRAJ23*01	CGNQGGKLIF	T G T G C T G G G A A C C A G G G A G G G A A A G C T T A T C T T C
SFW	TRAV21*02	TRAJ23*01	CGNQGGKLIF	T G T G C T G G G A A C C A G G G A G G G A A A G C T T A T C T T C

B

	TRBV (IMGT)	TRBV (IMGT)	CDR3 β (aa)	CDR3 β (nt)
UTT	TRBV12-3*01	TRBV12-1*01	CASSLAIDEQFF	T G T G C C A G C A G T T T A G C G C T G G A T G A G C A G T T C T T C
UBV	TRBV12-3*01	TRBV12-1*01	CASSLAIDEQFF	T G T G C C A G C A G T T T A G C G C T G G A T G A G C A G T T C T T C
JZX	TRBV12-3*01/TRBV12-4*01	TRBV12-1*01	CASSLAIDEQFF	T G T G C C A G C A G T T T A G C G C T C G A T G A G C A G T T C T T C
SFW	TRBV12-3*01/TRBV12-4*01	TRBV12-1*01	CASSLAIDEQFF	T G T G C C A G C A G T T T A G C G C T T G A T G A G C A G T T C T T C

Figure 5 - figure supplement 2 TCR sequencing of B*35/FVS-sorted samples

Nucleotide alignment of the CDR3 α and β sequence of PBMCs sorted on B*35/FVS-tetramer binding. Segment numbering is depicted according to the international immunogenetics information system (IMGT) nomenclature. A) Nucleotide alignment of the CDR3 α sequences. B) Nucleotide alignment of the CDR3 β sequences.